minerals

MDPI

Article

Coal Sludge Permeability Assessment Based on Rowe Cell Consolidation, and Filtration Investigations

Justyna Adamczyk [1] **and Radosław Pomykała** [2,*]

[1] Department of Geomechanics, Civil Engineering and Geotechnics, Faculty of Civil Engineering and Resource Management, AGH University of Science and Technology, 30-059 Krakow, Poland; jadamcz@agh.edu.pl
[2] Department of Environmental Engineering, Faculty of Civil Engineering and Resource Management, AGH University of Science and Technology, 30-059 Krakow, Poland
* Correspondence: rpomyk@agh.edu.pl

Abstract: In this paper, an attempt has been made to investigate the possibility of using coal sludge to seal a landfill site by presenting the results of their compressibility and permeability tests. Coal sludge is a fine-grained waste from the coal enrichment process, and its permeability is also highly dependent on its degree of consolidation. The tests were carried out in a Rowe Cell, making it possible to determine the water permeability coefficient more precisely by determining the degree of the material consolidation during testing. The test was carried out using backpressure conditions. The test procedure in the Rowe Cell consisted of the following three steps: saturation, consolidation, and filtration. The coal sludge was taken directly from the filter presses as a by-product of the fines' coal enrichment process. The paper presents the results of the individual stages performed in a Rowe Cell. The consolidation coefficient was determined using three different methods (Casagrande, Taylor, and Robbinson methods). The permeability coefficient was measured by the indirect and the direct method, the results of both were compared. The results ($k < 10^{-9}$ m/s) indicated that the value of the permeability coefficient responds to the value for isolating barrier materials.

Keywords: coal sludge; Rowe Cell; saturation; consolidation; filtration; coefficient of permeability; backpressure conditions

Citation: Adamczyk, J.; Pomykała, R. Coal Sludge Permeability Assessment Based on Rowe Cell Consolidation, and Filtration Investigations. *Minerals* **2022**, *12*, 212. https://doi.org/10.3390/min12020212

Academic Editors: Francisco Franco, Michael G. Stamatakis and Manuel Pozo Rodríguez

Received: 23 December 2021
Accepted: 24 January 2022
Published: 7 February 2022

1. Introduction

Many studies are focusing on investigations into the properties of coal wastes, which are important for use in geoengineering applications. However, most of them are concerned with rock waste, i.e., medium or coarse grain material [1–10]. Fine-grained waste from the coal enrichment process depends on the processing technology, flotation waste, or coal sludge (CS). These wastes are more difficult to manage than medium and coarse-grained wastes due to higher humidity (the enrichment process takes place in the aquatic environment) and, often, the content of combustible parts.

Coal sludge (CS) is a material that, due to the high content of combustible parts, is most often considered in terms of its use in the power industry. The research work has mainly focused on determining the possibility of using coal sludge as a potential energy fuel as a low-energy raw material for combustion in boilers [11–13]. Research is also underway on its use for the production of artificial aggregates [14], bricks [15,16], additives to other thermal processes [17], backfilling material [18], ecological mixtures that will be used for the reclamation of land degraded by industry [6,19], as well as the possibility of using ashes after burning coal sludge [20].

However, attention should be paid to the fact that apart from about 20–50% [11–13,21,22] of combustible particles, the remaining content of coal sludge is mineral materials (mainly: chlorite, kaolinite, minerals from the mica group, quartz, smectite-illite packages). Hence, the possibility of using coal sludge waste in another direction, such as geoengineering, should

be considered, taking advantage of its geotechnical properties, given the fact that it is still a waste considered challenging to use.

Because the use of fine-grained tailings in geoengineering is much more prevalent in the case of flotation tailings from ore processing [23,24], and not for coal, it is all the more worth exploring. The research on the properties of coal sludge waste is currently mainly focused on analyzing its filtration and physicomechanical parameters [19,25–27] but geotechnical properties of flotation wastes from hard coal processing (e.g., consistency limits, strength and deformation parameters) become at present more often the subject of scientific research [1,2,4,27–30].

One of the possibilities of using coal sludge is to use it for sealing municipal landfills. Klojzy-Kaczmarczyk and Staszczak [31] conducted extensive analysis to determine the demand for the material to be used in the construction of insulating layers of such facilities. It encompassed three voivodships (provinces), Opolskie, Śląskie, and Małopolskie, for which the total demand for coal sludge as insulating layers was estimated at approx. 2.7 million Mg. The analysis was an initial recognition of possibilities to apply coal sludge for sealing waste storage sites. The recognition is complemented by the studies of the permeability coefficient for coal sludge and its physical-mechanical and chemical properties. In the studies conducted so far on the filtration properties of coal sludge, the values of the filtration coefficient are within 10^{-9}–10^{-11} m/s [28,31,32]. Therefore, according to the current classifications at poor compaction, it is a material (10^{-9} m/s) that can be considered as a poorly insulating raw material [33,34] or with average vertical permeability (according to [35]).

The aim of the paper is to investigate the permeability of coal sludge and present if coal sludge could be used as a material for isolation barriers in landfills layers. The paper presents the results of the individual stages performed in a Rowe Cell. First, full saturation of the sample was achieved using the equalizing pressure method. Next, consolidation of the material was carried out at a constant pressure gradient. Finally, the filtration coefficient was determined using both direct and indirect methods.

2. Theory Background

The full version of this section is available in the Supplementary Materials, including Tables S1 and S2.

2.1. Soil Consolidation

The theory of consolidation for a soil medium deals with the issues related to the change in pore water pressure in the soil, and the change in effective stresses, with a simultaneous decrease in the loaded zone of the soil. Consolidation is, therefore, the process of decreasing soil volume under the influence of a load applied due to the dissipation of excess water pressure and its outflow from the soil pores. Consolidation depends on the filtering properties of the soil and results in soil settlement ([35] after [36]).

The basic model of consolidation, according to Terzaghi, considers the ground as a two-phase medium (fully saturated state—the pores of the ground are filled with water—a state achieved in the process of saturation, which precedes consolidation). Thus, consolidation is a long-term process, and its duration depends on many factors. The theory of Terzaghi (1925) is the first solution to consider the rate of uniaxial consolidation of saturated soils [37]. Its assumptions and detailed analysis and solutions of the basic equation are presented by [38,39], among others.

2.1.1. Saturation

The saturation process aims to saturate the sample by filling all the pores in the ground with water. This process involves a gradual increase in water pressure in the soil pores to dissolve the air bubbles. This phenomenon is described by Henry's law [40]. For semi-permeable soils, gravitational saturation only slightly increases the water content in the sample. Therefore, to fill all pores with water is necessary to apply an equalizing pressure

(back pressure), which allows maintaining a constant value of effective stress in the sample during the saturation process. The parameter controlling the degree of sample saturation is the Skempton parameter, which defines the ratio of the increase in water pressure in the soil pores in the rise of the total pressure applied to the sample [41]. The values of this parameter are included in Table S1.

2.1.2. Characteristics of Soil Consolidation

The basic parameters describing the consolidation process are the time factor, the coefficient of dissipation of pore water pressure in the soil (degree of consolidation), and the consolidation coefficient.

The time factor is given to determine the average value of the consolidation degree of a given layer or to determine the value of the consolidation degree at a given depth. The value of the time factor depends on the consolidation ratio, time, and flow path. For example, when drainage occurs in both directions, the value of the time factor increases by a factor of four [36,42]. The dependence of variation of the time coefficient on the value of the consolidation degree is presented in tabular form by the same authors.

Degree of dissipation of water pressure in soil pores (degree of consolidation). British Standard BS 1377-6 1990 [43], defines the pore pressure dissipation rate in soil pores as the ratio of the pore pressure difference between the start of the consolidation phase, and the consolidation time, to the pore pressure difference between the start, and the end of the consolidation phase.

In the literature describing the consolidation process, the authors rarely refer to the degree of pore water pressure dissipation. In contrast, there appears the concept of consolidation degree [36–38,44], defined as the ratio of the difference between the excess pore water pressure at the beginning of the consolidation process, and the excess pore water pressure during the consolidation time to the initial excess pore pressure.

Consolidation coefficient c_v is a parameter that defines the speed of soil settlement. Its value generally decreases with increasing soil liquidity limit, and the range of variation of for a given liquid limit of soil is quite wide [38]. The consolidation coefficient c_v is used to calculate the value and rate of consolidation deformation of soils under load [45]. The value of the consolidation coefficient may be determined by the analytical method from the solution of Terzaghi's equation or by the use of empirical methods in which, for a given load increment of the tested sample, the characteristics of experimental and theoretical consolidation curves are compared, the so-called curve fitting process. Consolidation curves are more readable if the consolidation time is ploted on a logarithmic scale or presented as a square root [38].

Many literature sources distinguish two graphical methods for determining c_v under laboratory conditions in uniaxial consolidation tests [37,38]. One is the logarithmic-time method proposed by [46], and the other is the square root method suggested by [47]. In [42], in addition to the methods above, the third graphical method using the pore pressure dissipation factor is also defined. The general procedures for determining c_v by the methods mentioned earlier are included in Table S2.

2.1.3. Phases of the Soil Consolidation

Immediately after the load is applied to a cohesive soil, due to the movement of free water molecules to more firmly bound water zones, the pore pressure in pore-filling water increases, and it takes up the entire load increment. The excess water is squeezed out of the higher-pressure areas into the lower-pressure areas. This process continues until the pore water pressure in the soil is equalized, there is no outflow of water from the sample, no displacement of soil particles, so no consolidation occurs.

When the drainage is unblocked, the water moves out of the loaded zone (filtration consolidation), with a simultaneous increase in the effective stress of the soil skeleton. When the structural strength of the soil is exceeded (up to 0.15 MPa), the pore pressure increases again; water is squeezed out of the pores (structural consolidation). When the

consolidation process is complete, the pore water pressure equals the hydrostatic pressure that existed before the soil load was increased. Thus, the effective stresses increase by the whole increment of soil pressure.

Many researchers have observed that the different phases of deformation overlap and proceed simultaneously—the phase of deformation associated with structural consolidation already occurs during filtration consolidation [36,48,49].

2.2. Soil Water Permeability

2.2.1. Movement of Water in the Ground

Under natural conditions, the water flow in the ground is caused by the earth's gravitational forces, which tend to level off the differences in the level of water in the ground [49]. Thus, the movement of water in the ground can be determined or undetermined in time [34,50]. The motion in which water particles in adjacent layers move parallelly to each other and the direction of the water flow is referred to as laminar motion. The basic law on which the dynamics of water flow in porous media is based, assuming laminar motion, is Darcy's law, also called the linear filtration law [50].

The assessment of filtration properties is also related to the direction of water movement in the soil. The three basic directions of water movement in nature are horizontal, vertical downwards, and vertical upwards. Horizontal water flow is usually found at the top of an impermeable layer. The vertical downward flow usually occurs when the seeping of sub-soil water through the layer of low permeable soil below takes place, while the vertical upward flow occurs when pumping water from the bottom of the excavation as well as during construction works in the low permeable layer, the bottom of which is under the pressure of the interstitial water present below. Water permeability of soils is the ability of water to pass through the network of channels formed by the pores of the ground. The measure of water permeability of the ground is the filtration coefficient (water permeability coefficient), which according to Darcy's filtration law defines the relationship between the hydraulic gradient, and the speed of water flow through the pores of the ground [49].

The physical properties of the flowing water that affect the water permeability of soils are its temperature, viscosity, specific gravity, mineralization, soil texture as well as methods and conditions of measurements [34].

2.2.2. Methods for the Determination of the Filtration Coefficient

The value of the filtration coefficient is determined based on empirical and analytical formulas), laboratory, and field tests, as well as mathematical, physical, and numerical modeling.

The choice of the method for determining the filtration coefficient depends, to a large extent, on the size of the grains, particles, and the associated properties of the soil under investigation. Permeability coefficient determination methods can be divided into the following:

- analytical and empirical formulas based on the grain size distribution (Hazena, and Kozeny-Carman formulas [51,52]; Hazen, Slichter, Terzaghi, Beyer, Sauber, Krueger, Kozeny, Zunker, Zamarin, USBR, Alyamani, and Sen, Shepherd, and Loudon [53]; Terzaghi, Kozeny, Carman, Zunker, and Chapuis [54–56]; Hazen [57]; Kruger [58]),
- laboratory and field tests (in situ permeameter test [59]; Filtration Column [58]; ZWKII apparatus [60]; Oedometer [61], Rowe Cell [39,62])
- modelling (mathematical, physical, numerical: using DEM [51]; Using FEM [20]; Using LEM, FEM [61]).

2.2.3. Laboratory Tests

Laboratory methods for the determination of the filtration coefficient should model the main directions of water flow in the soil. The flow rate measurement methods used in laboratory studies can be divided into direct and indirect methods (taking into account both constant and variable hydraulic gradient). A list of instruments used in individual

methods is presented by [48]. Due to their granulometric composition, the studies on water permeability of fine-grained wastes such as coal sludge should be carried out by the methods designed for cohesive soils in devices such as triaxial apparatus, consolidometers (e.g., Rowe Cell), or specially adapted edometers. The construction and operation principles of the most commonly used instruments for determining the coefficient of permeability of semi-permeable formations are exhaustively described in the following publications [63–65].

3. Materials and Methods

3.1. The Origin of the Samples

Coal sludge comes from a hard coal mine located in Poland in the Upper Silesia region. Coal sludge is a by-product of enrichment of hard coal with a fraction size of 0–2 mm in coal separators or in the flotation process. The sequence of the process of coal sludge formation as well as the location of the bulk sample of coal sludge for testing was filter presses (Figure 1).

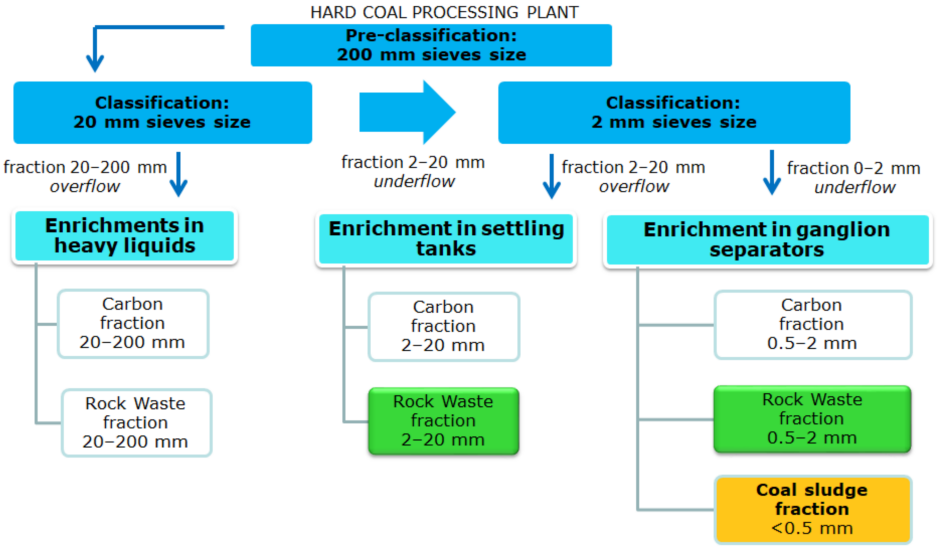

Figure 1. The process of formation of coal sludge.

The coal sludge was taken directly from the filter presses, a by-product of the enrichment process of coal fines (fraction < 0.5 mm). Currently, the primary direction for managing this material is to use it as a low-energy raw material for combustion in boilers [51]. Research is also underway for its use in the production of ecological mixtures to be used for the reclamation of land degraded by industry. Despite this, very large amounts of this material are still deposited in the settling tank. The test material was taken from the averaged sample (except for mineralogical and petrographic properties tests, where five samples were taken, before averaging).

CS samples intended for research in the Rowe Cell were brought to the optimal moisture and the corresponding maximum dry density of the soil skeleton. Samples prepared in that way were put into Rowe Cell.

3.2. Coal Sludge Characteristic

The following part presents the characteristics of the tested material, which takes into account the properties that may affect the value of the filtration coefficient. The set consisted of tests of the following basic properties: grain composition; chemical composition; optimal moisture; environmental properties: leachability of chemical contamination and radionuclide content; as well as mineralogical and petrographic properties: the microscopic analysis and phase composition.

Grain composition was determined using the particle analyzer Analysette 22 laser particle meter by Fritsch (Markt Einersheim, Germany).

The test of optimum moisture content was carried out in accordance with the standard EN 13 286-2:2010 [66].

The chemical composition, trace element content and leachability tests were carried out in accordance with the PN-EN 12457-4 standard [67] with use a mass spectrometer (ICP-MS) and an emission spectrophotometer (ICP-OES). The tested samples were digested with HNO3/HCl and a microwave mineralizer. The tests of were carried out in the AGH-UST laboratories. Obtained results were compared with allow values specified in the relevant regulations [68,69].

The standard scope of tests of the content of radionuclides includes, for waste material, tests for the content of trace elements, leachability of chemical pollutants and the content of the following natural radioactive isotopes: potassium K-40, radium Ra-226, and thorium Th-228 track. The specific activity of radioactive isotopes contained in the coal sludge was determined in accordance with the guidelines contained in the [70].

The microscopic examinations were performed using the universal Olympus BX51 polarizing microscope. Observations were made in transmitted light on polished microscopic slides (thin plates) with a thickness of 0.03 mm. The preparations were impregnated with epoxy resin before preparation. Magnifications from about 100 to 250 times were used.

The microscopic analysis was supplemented with phase composition tests performed with the X-ray method (XRD). In order to check the homogeneity of the samples, 5 analyses were performed for each of them. X-ray tests were performed on standard powder formulations on the RIGAKU SmartLab diffractometer (Austin, TX, USA) with the following measurement parameters: CuKα radiation, graphite reflective monochromator, lamp voltage 45 kV, lamp current 200 mA, measuring step 0.05°2θ, pulse counting time 1 s/step.

3.3. Laboratory Testing Program

3.3.1. Testing Apparatus

The Rowe Cell is a device designed to allow complete saturation of the sample, arbitrary load setting, outflow of water in different directions, measurement of water pressure in soil pores, and water flow rate in the sample. The main functions of the device are testing the consolidation, and permeability in vertical, and horizontal directions of fine-grained soils characterized by low filtration coefficient. The test procedure is detailed in [43], the test conditions are shown in Figure 2.

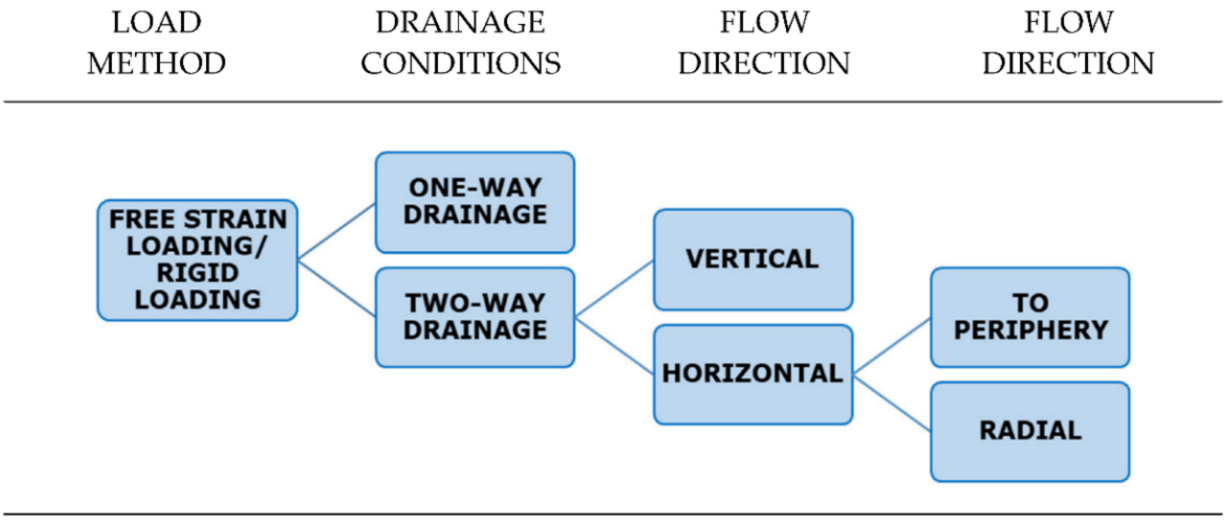

Figure 2. Conditions for drainage, load, and flow direction for consolidation, and permeability tests in Row cell.

The Rowe Cell is equipped with a hydraulic system for setting the vertical load in the cell. The main component of the apparatus is a chamber composed of the following three parts: the chamber proper (body), the cap, and the base. Tests were carried out on the VJT0640 model from VJTech (Berkshire, United Kingdom), with a maximum acceptance pressure of 1000 kPa [71].

The body, made of stainless steel, is fitted between the cap, and the base of the chamber. The inner side of the side surface of the body, in its upper part, is provided with a filter connected to a valve fixed to the central part of the side surface on the outer side of the chamber. This system forms the drainage used for determining the horizontal coefficient of consolidation, and the horizontal coefficient of permeability (Figure 3, point F).

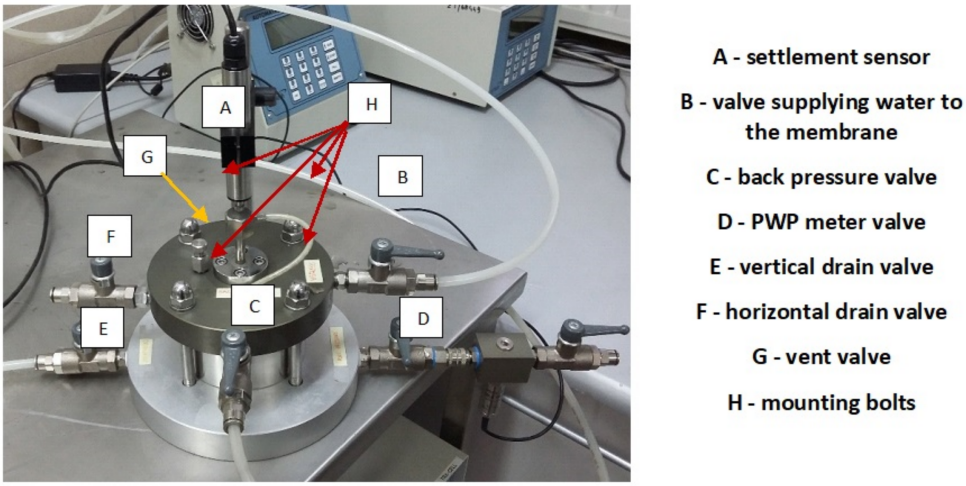

Figure 3. Construction of the Rowe Cell apparatus—valves location.

The cap of the chamber is equipped with a rubber membrane and a drainage stem. Two valves lead out of the side surface of the cap and supply water to the diaphragm and the drainage stem. The valves are connected to pressure pumps, which are the pump for vertical pressure on the sample (Figure 3, point B), and a pump regulating the equalizing pressure inside the sample (Figure 3, point C), respectively. A vertical settling sensor (Figure 3, point A) attached to a tripod is attached to the cap. Additionally, apart from the holes for four fastening screws located on its periphery in the chamber cap, there is also a valve for venting the system (Figure 3, point G).

The base of the chamber has a circular recess in which an o-ring is inserted to act as a seal between the base, and body of the chamber. In the central part of the chamber base, there are two drainage holes, which are connected to respective valves located on the opposite sides of the chamber base. One valve forms the drainage used in determining the vertical consolidation ratio (Figure 3, item E), the other is connected to the pore pressure transducer (Figure 3, item D). The individual parts of the chamber are joined by four fastening screws (Figure 3, point H).

Three hydraulic pressure pumps are used in the test, as follows: the first is to apply a vertical load to the sample in the consolidation chamber, the second is to control the equalizing pressure, and the third is for two-directional flow conditions and permeability coefficient determination. The process is controlled by a computer program, in which desired pressures are set for the different stages of the test. The parameters measured during the test are settlement and pore water pressure.

3.3.2. Testing Procedure

The test was carried out under equalizing pressure conditions. The test procedure in the Rowe Cell consists of the following three steps: saturation, consolidation, and filtration of the sample.

Saturation

The procedure of testing in the Rowe Cell assumes that the degree of saturation of the sample Sr during the saturation process reaches a value of 1. The full saturation of the soil pores allows for the determination of effective stresses, which determine the strength of the soil. The sample is placed in a constant pressure chamber. Porous filters are placed on the upper, and lower surfaces of the sample to ensure that the pore pressure in the sample is evenly distributed. Ventilation of the sample is carried out under conditions of isotopic consolidation $\sigma_1 = \sigma_3$. After each stage of increasing the pressure in the chamber, the degree of saturation of the soil must be checked. For this purpose, the Skempton parameter (1) is used [40]:

$$B = \frac{\Delta u}{\Delta \sigma_1} \quad (1)$$

The saturation stage includes two processes, which are carried out alternately until the sample is saturated. The first one is the control of the sample saturation degree. It consists of increasing the chamber's pressure by a small value, reading the increase in the water pressure inside soil pores, and determining the value of the Skempton B parameter, which determines the degree of filling the pores of coal sludge with water. The second process is to saturate the sample with water. This process was carried out in a constant stress increment mode (5 kPa/h). These stages are repeated until the required value of the B parameter is reached.

The saturation process occurs under constant effective stress, which was 15 kPa/10 kPa/10 kPa for samples CS1, CS2, and CS3, respectively. The saturation stage ended when the value of the Skempton parameter reaches B = 1 Figure 4.

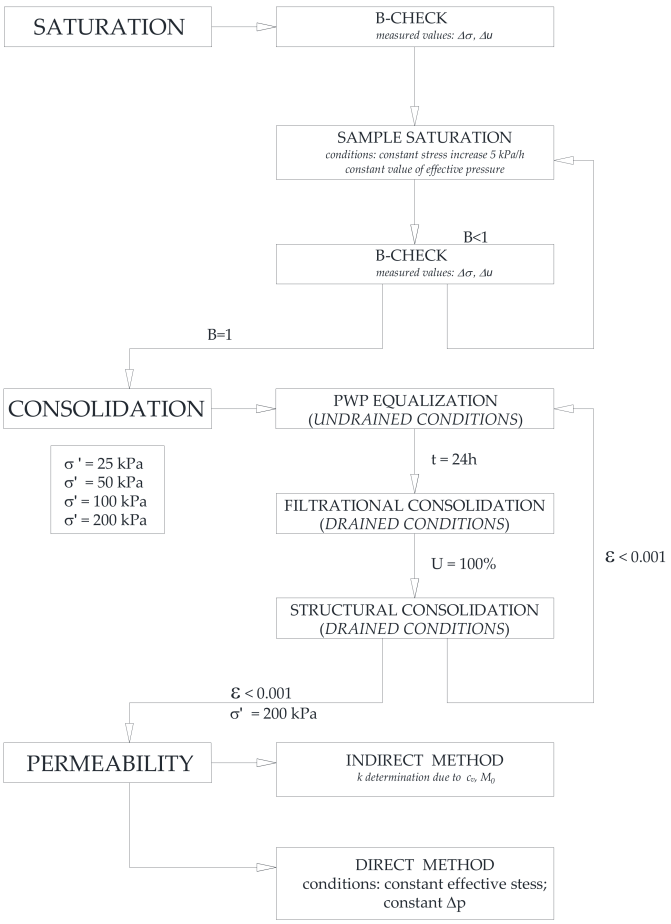

Figure 4. The Rowe Cell investigation algorithm.

Consolidation

In the Rowe Cell, the consolidation process was performed for four loading degrees, with each successive pressure being twice as high as the previous one. Thus, the effective stresses in the next loading degrees were 25 kPa, 50 kPa, 100 kPa, and 200 kPa. Each loading degree consisted of the following three stages: equalization of pore water pressure in soil pores (under conditions without the possibility of water outflow from the sample, stabilization time 24 h), filtration consolidation (drainage of the sample until the pore pressure dissipation factor reached U = 100%), and structural consolidation (during which the sample, after water outflow from it, remained under a given load until the vertical deformation stabilized: $\varepsilon < 0.001$). Consolidation took place under constant equalizing pressure (the pressure on the membrane was increased because, due to the saturation of the sample, the tested system had a two-phase nature, as follows: solid medium and water, which caused a direct increase in effective stress) Figure 4.

The following measurements were carried out during the test, as follows: total pressure in the chamber, pore water pressure in the soil, effective pressure, vertical displacement, and volume changes of the flowing water. In addition, the values of the consolidation factor were determined by plotting consolidation curves using the Casagrande, Taylor, and Robbinson methods (method of pore pressure dissipation factor).

Permeability

Determination of the permeability coefficient for coal sludge has been carried out using an indirect method (using correlations with the consolidation coefficient), and a direct method in which measurements were carried out under conditions of a constant hydraulic gradient, with the vertical direction of the filtration stream as follows: from top to bottom. During the test, the following data were recorded by the software as follows: vertical pressure applied to the chamber, equalizing pressure, the pressure of water flowing out of the sample, the pressure of water in soil pores, vertical displacement of the sample, the volume of water flowing into the sample, the volume of water flowing out of the sample.

The study was conducted in the following two options:

1. fixed effective stress σ'_n= 200 [kPa], with four different pressure gradients Δp (40, 60, 80, 100 kPa)
2. constant pressure gradient, with two different effective stress σ'_n= 250 [kPa] and σ'_n = 300 [kPa]: Δp = 40 kPa—samples: CS2, CS3, Δp = 100 kPa—sample CS1.

Detailed conditions for the water permeability determinations are shown in Figure 5.

The Student's t distribution was used to estimate the confidence interval of the compressibility coefficient c_v, and the permeability coefficient k determined at individual vertical stresses, including the true value of the parameter at the assumed confidence factor $(1 - \alpha) = 0.99$, due to the small sample size ($n = 9$).

A test for two variances was used to verify whether the values of the permeability coefficient obtained by the indirect and direct methods are the same. At the significance level $\alpha = 0.05$, the hypothesis was tested, the mean values of the filtration coefficients obtained by the direct method and by the indirect method at Δp = 40 kPa are the same. Based on the values of the filtration coefficients $H_0 : \sigma_1^2 = \sigma_2^2$, the hypothesis was tested against the alternative $H_1 : \sigma_1^2 > \sigma_2^2$ hypothesis.

3.3.3. Specimen Preparation

The specimens, measuring 75.7 mm in diameter and 50 mm in height, were cut from material with an optimum moisture content of 27.8% and compacted to ρ_{dmax} = 1.458 g/cm^3. Three specimens were assigned to the tests. The first one, immediately after preparation, was placed in a Rowe Cell and tested. The remaining specimens, having been properly protected against water loss, were stored at 4 °C.

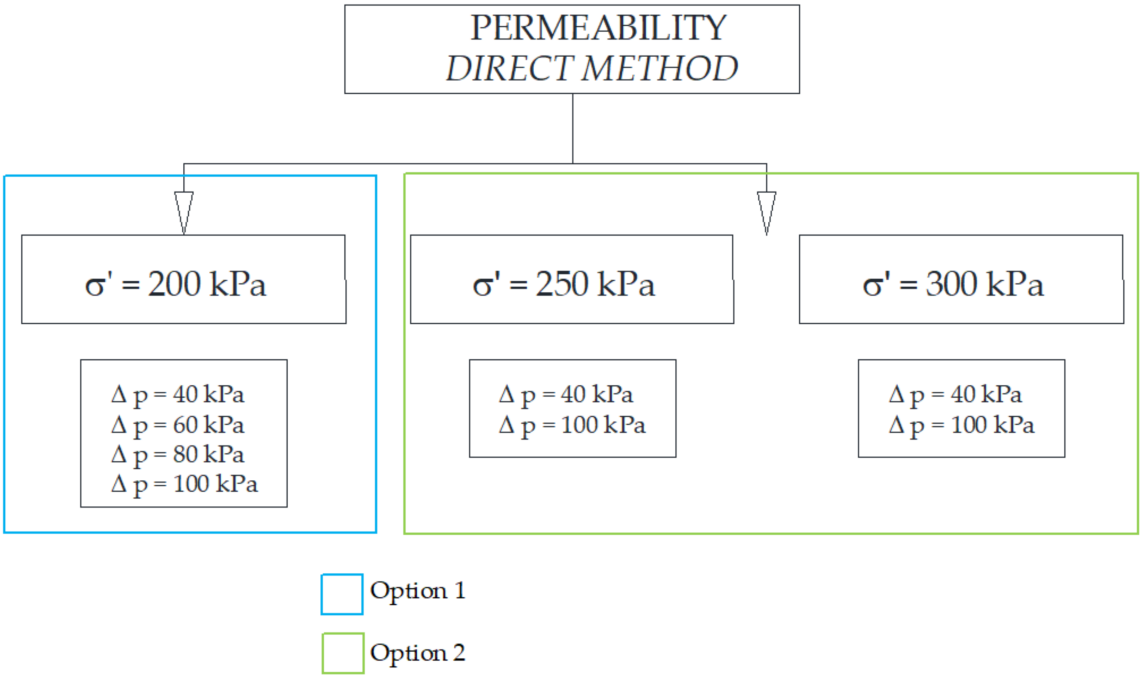

Figure 5. Variants of the conducted permeability tests (direct method).

4. Results and Discussion

4.1. Material Characteristic

4.1.1. The Grain Composition

The total content of the clay, and silt fraction (88%), and the 12% share of the sand fraction read from the granulometric composition curve (Figure 6) according to the guidelines of [72] classify the coal sludge (CS) as silty clay (siCl). This particle size distribution is typical of fine-grained waste from hard coal processing [18,22,31].

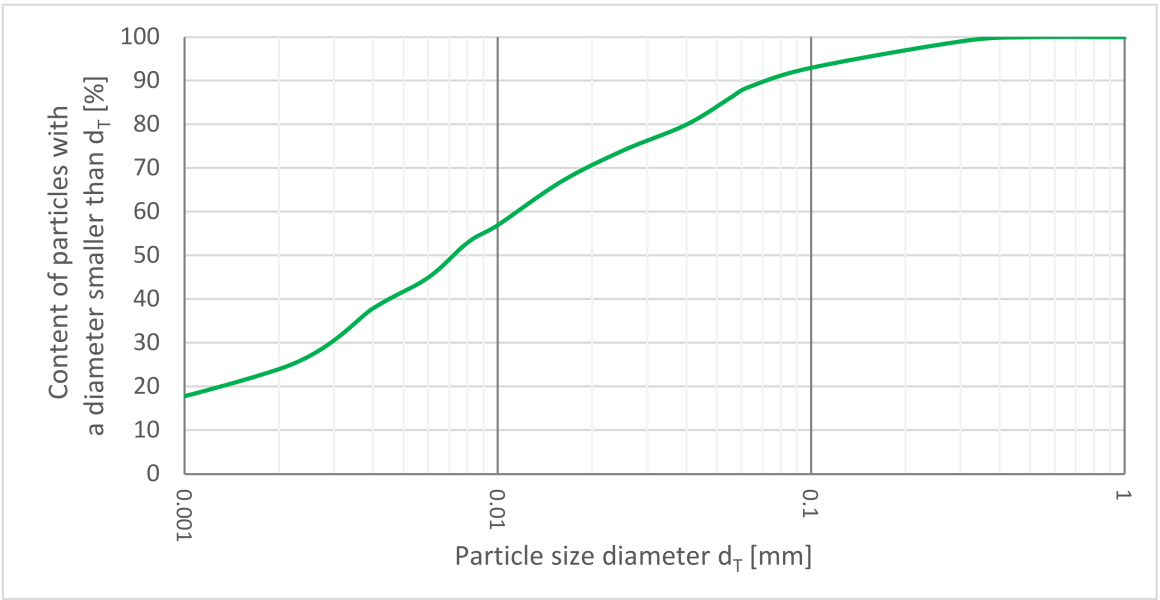

Figure 6. Coal sludge grain size curves.

4.1.2. The Chemical Properties

The main chemical components present in the coal sludge are silicon and aluminum. Their contents are 33.5% (SiO_2) and 21% (Al_2O_3), respectively. A summary of the chemical composition is provided in Table 1. The chemical composition results directly from the composition of the rocks accompanying the coal seams in Poland. The LOI value is typical for this type of waste. is in the average test content indicated by various researchers [11–13,22].

Table 1. The chemical composition of the coal sludge [73].

Ingredient	Percentage [%]	Ingredient	Percentage [%]
P_2O_5	0.10	CaO	0.26
Mn_2O_5	0.02	MgO	0.61
SiO_2	33.50	Na_2O	0.53
TiO_2	0.02	Li_2O	0.01
Al_2O_3	21.00	K_2O	1.10
Fe_2O_3	3.76	SO_3	0.89
LOI *	38.2		

* loss of ignition (at 800 °C).

4.1.3. The Optimum Moisture

The optimum moisture content of waste coal sludge was determined based on three series of tests; its value remains in the range 26–29.4% and the average value is 27.80% (Figure 7). The maximum volumetric density of the ground skeleton ranged from 1.441 g/cm^3 to 1.48 g/cm^3 (mean value 1.458 g/cm^3).

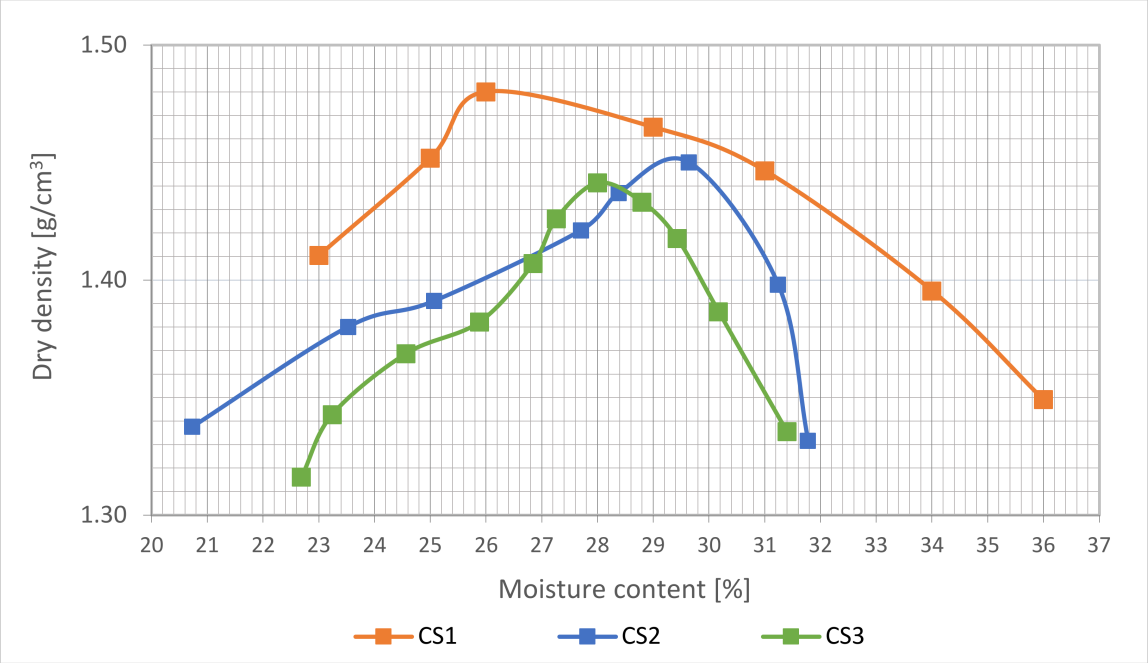

Figure 7. Coal sludge compressibility curve.

4.1.4. The Trace Element Content and Leachability of Chemical Impurities

The results of the direct analyses of the coal sludge (CS), showing the content of trace elements and the leachability of chemical impurities from the tested materials, are presented in Tables 2 and 3, respectively. Coal sludge meets the environmental requirements in terms of the maximum content of substances particularly harmful to the aquatic environment, permissible concentrations of pollutants in soils belonging to the land.

Table 2. The contents of trace elements in the coal sludge [73].

No.	Parameter	Result [ppm]	No.	Parameter	Result [ppm]
1.	Zinc (Zn)	62.54	7.	Nickel (Ni)	19.25
2.	Barium (Ba)	239.56	8.	Lead (Pb)	19.64
3.	Cadmium (Cd)	2.07	9.	Molybdenum (Mo)	2.20
4.	Cobalt (Co)	6.20	10.	Tin (Sn)	8.14
5.	Chromium (Cr)	56.98	11.	Arsenic (As)	2.58
6.	Copper (Cu)	24.55	12.	Mercury (Hg)	0.01

Table 3. The leachability of chemical impurities from the coal sludge [73].

Indicator	[mg/dm^3]	* [mg/dm^3]	Indicator	[mg/dm^3]	* [mg/dm^3]
pH	9.19	6.5–9	Lead	<0.0002	0.5
Sodium	197.30	800	Mercury	<0.0001	b.w.
Potassium	6.75	80	Cadmium	<0.00003	b.w.
Beryllium	<0.00001	1	Selenium	<0.020	1
Calcium	10.48	b.w.	Antimony	0.00210	0.3
Magnesium	10.22	b.w.	Aluminum	0.020	3
Barium	0.009	2	Chromium	0.0130	0.5
Strontium	0.090	b.w.	Molybdenum	0.0003	1
Manganese	0.020	b.w.	Titanium	<0.002	1
Zinc	<0.0010	2	Arsenic	0.001	0.1
Copper	0.0025	0.5	Thallium	0.0005	1
Nickel	<0.00001	0.5	Chlorides	295.0	1000
Cobalt	0.00054	1	Sulfates	59.6	500

* Acceptable values according to [71]; b.w.—no value.

4.1.5. The Radioactivity

The specific activity of radioactive isotopes contained in the coal sludge was determined in accordance with the guidelines contained in the [70]. Coal sludge meets the environmental requirements in terms of the content of natural radioactive isotopes of potassium (40 K), radium (226 Ra) and thorium (228 Th) in raw materials and materials construction, specified in the relevant regulations. The contents of radioactive elements are given in Table 4.

Table 4. The concentrations of natural radioactive isotopes in the coal sludge [73].

Sample Designation	Specific Activity		
	^{40}K	^{226}Ra	^{228}Th (^{228}Ra)
	[Bq/kg]	[Bq/kg]	[Bq/kg]
Coal sludge (CS)	511 ± 30	76 ± 5	68 ± 5

4.1.6. The Mineralogical and Petrographic Properties

The microscopic analysis

Coal sludge is a black material, which in the dry state is cohesive and brittle, while in the moist state is plastic. It is made of silt and clay fractions mainly [73].

The microscopic analysis revealed sharp-edged, opaque coal crumbs sized 0.01–0.5 mm (dark brown) and a few fragments of "sporulation spores" (yellow or orange). The total share of these ingredients exceeds 40% of the sample volume. The sample shows a high content of grains smaller than 0.1 mm (Figure 8). Smaller amounts of grains of quartz and sharp-edged feldspar, up to 0.05 mm in size are visible, chaotically dispersed in the background. The ingredients are surrounded by an abundant, very finely grained clayey matrix containing scattered fine grains of coal dust and pyrite [73].

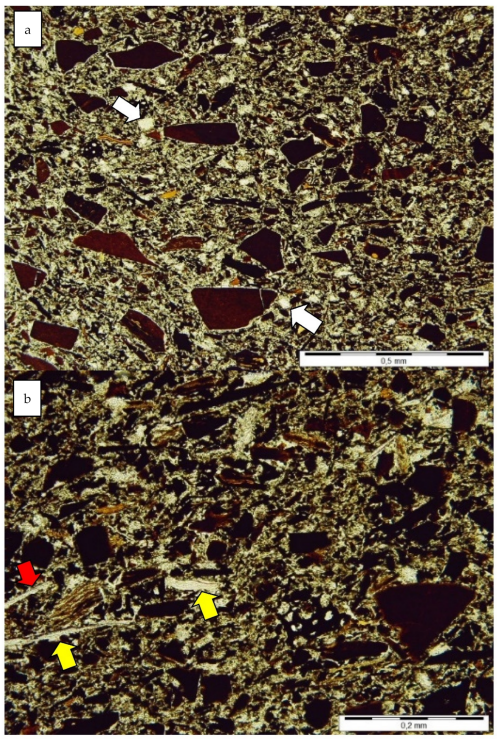

Figure 8. Microscope images of coal sludge (micrograph: one polarizer) [73]. (**a**) Coal Sludge (**b**) Mika plates.

The phase composition

The phase composition of the coal sludge consists mainly of clay minerals (Figure 9). The X-ray analysis of five samples found kaolinite, illite, chlorite (up to 5 %w) and mixed-packet minerals—smectite–illite (this is indicated by the widening of the lower part of reflex 10 Å). All the samples contained quartz (very strong reflections even at low contents, about a dozen or so percent by weight), mica (in small quantities), as well as small amounts of feldspar (1–3 %w), pyrite and halite (in sample 5). The phase compositions of the samples were very similar In addition, the presence of carbon was also observed in the material—the noticeable increase in the background of the X-rays within the 20–30°2θ range indicates presence of an amorphous phase [73].

4.2. Saturation

As a result of the saturation process, all three coal sludge samples were fully saturated with water; for each of the samples, the final value of the Skempton parameter was B = 1. However, some differences were observed in the saturation process itself for the individual samples. The discrepancies concerned the duration of the saturation process and the rate of increase in the Skempton parameter value (Figure 10).

The first sample (CS1), immediately after preparation, was placed in a chamber and subjected to saturation. The initial value of the Skempton parameter was B = 0.88. The saturation process lasted 2560 min. After this time, the degree of saturation of the sample was rechecked, and its value was B = 1. Thus, saturation was considered to be completed, and the consolidation stage started.

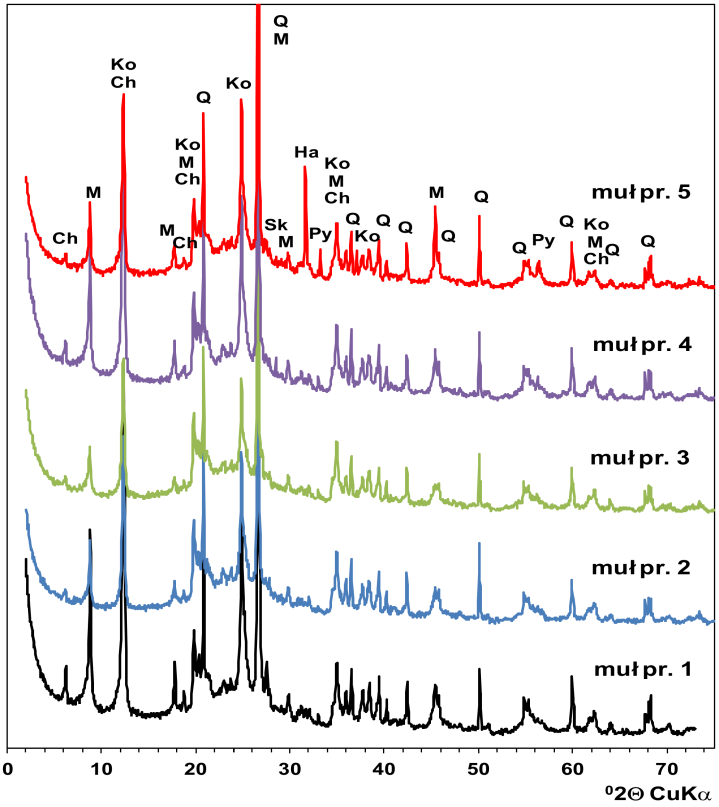

Figure 9. The X-rays of the coal sludge samples. Explanatory notes: Ch—chlorite, Ko—kaolinite, M—minerals from the mica group, Q—quartz, Py—pytite, Ha—halite, Sk—feldspar [73].

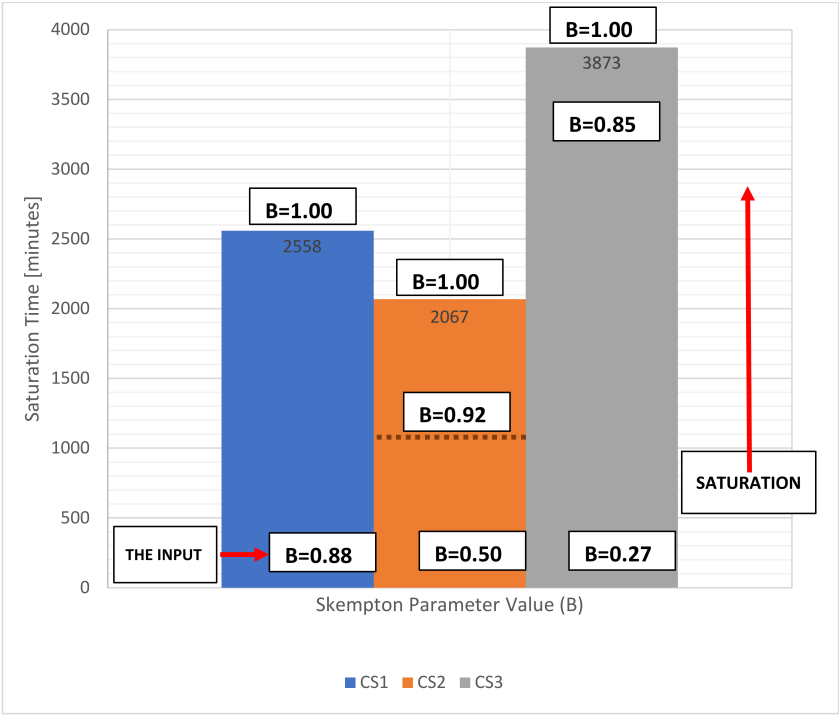

Figure 10. Comparison for an increase in the Skempton Parameter Value in time for tested samples.

The initial value of the Skempton parameter for the second sample (CS2) was B = 0.5. The sample was saturated in two stages; after 1000 min, the Skempton parameter was

B = 0.92; after another 1060 min, the saturation process was completed (B = 1), and the sample consolidation started.

The saturation time for the third sample (CS3) was 3872 min. The degree of saturation of the sample at the beginning of the test was much lower than for the other two samples and amounted to B = 0.27. The saturation was carried out in two stages. After 3270 min, Skempton's parameter achieved B = 0.85. In the next saturation stage, which lasted 602 min, full saturation of the sample was obtained (B = 1), and the saturation process was completed. The consolidation stage started. The course of the saturation process for CS1 is shown in Figure 11 (individual waste coal sludge CS2 and CS3 is shown at complementary materials).

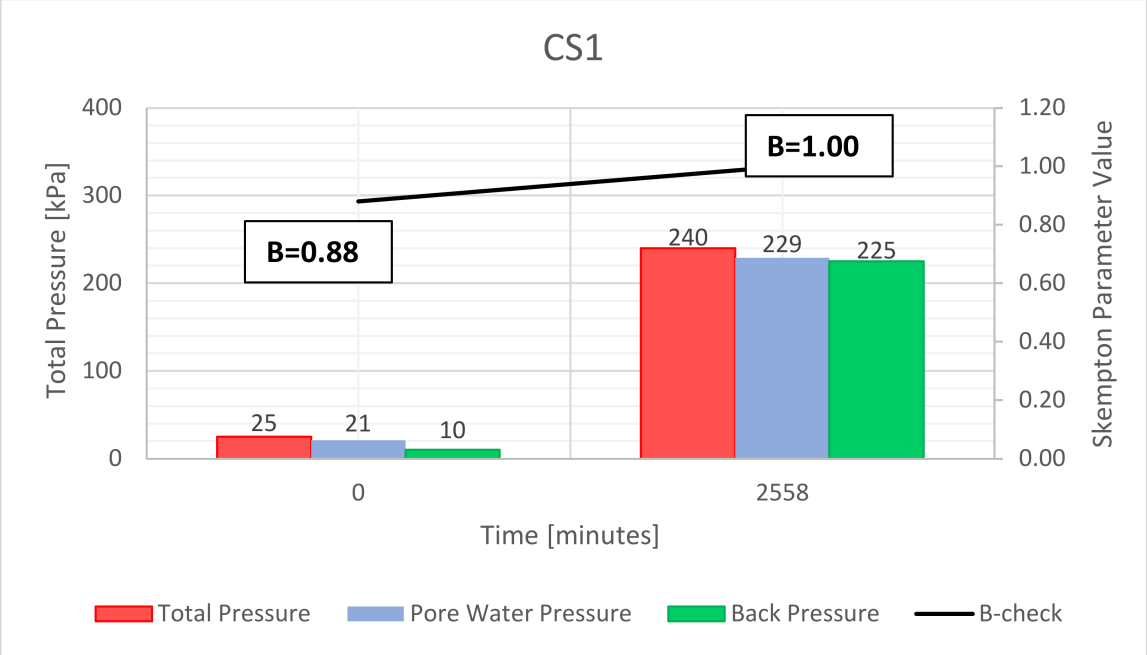

Figure 11. Coal sludge saturation process.

4.3. Consolidation

According to the procedure outlined in Section 3, consolidation was carried out for four load degrees. The first degree in each stage of the consolidation process was to equalize the pore water pressure in the soil. Next, the load was applied to the specimen under conditions that prevented water outflow, increasing pore water pressure, and subsequent stabilization of pore water pressure over time. The pore pressure stabilization time of 24 h was assumed. When the pores are filled with water and outflow is prevented, the applied load increases pore water pressure, while the effective stress increases only slightly (Figure 12).

Initially, the resulting excess water pressure in the soil's pores is not uniformly distributed but evens out over time. The greater the load increase on the sample, the greater the value of the water overpressure, and the longer the time required for the water pressure in the soil's pores to dissipate uniformly. The pore pressure rise curves and its stabilization in time for sample CS1 are shown in Figure 13.

It should be noted that the process of water pressure leveling in the soil pores in all three samples proceeds in a similar way, which also proves that the saturation was carried out correctly. Figure 14 shows the proportion of effective pressure and pore water pressure in the soil for individual samples at a total load increment of 100 kPa.

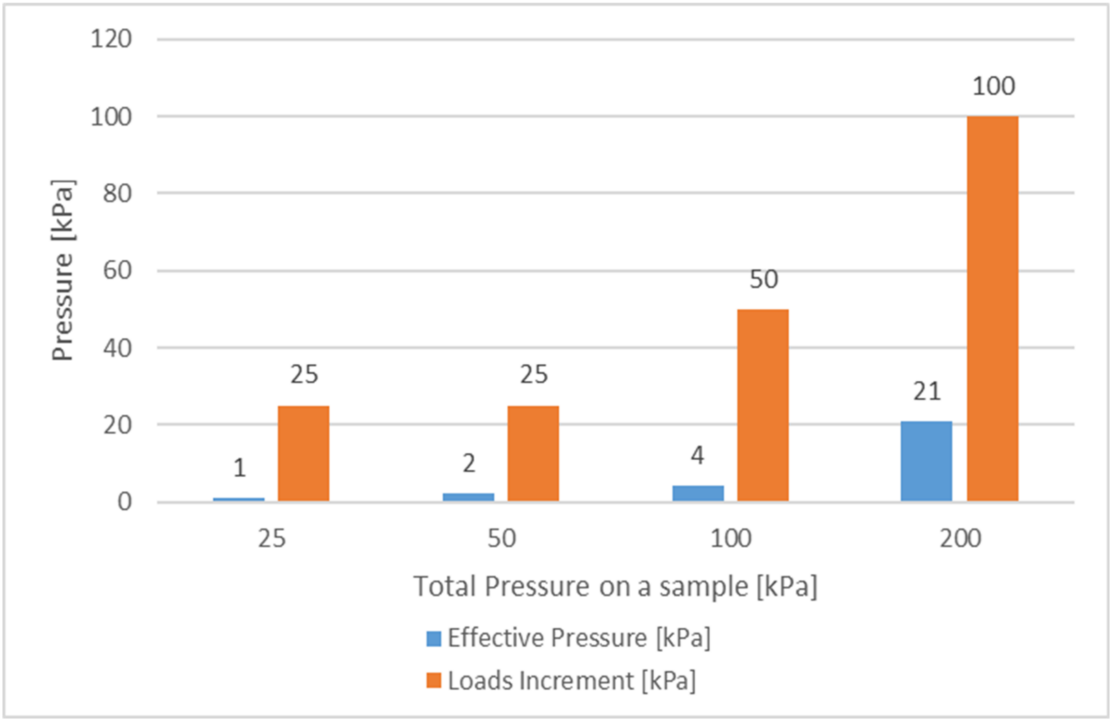

Figure 12. The participation of effective pressure in the following degrees of sample CS1 loading (undrained conditions).

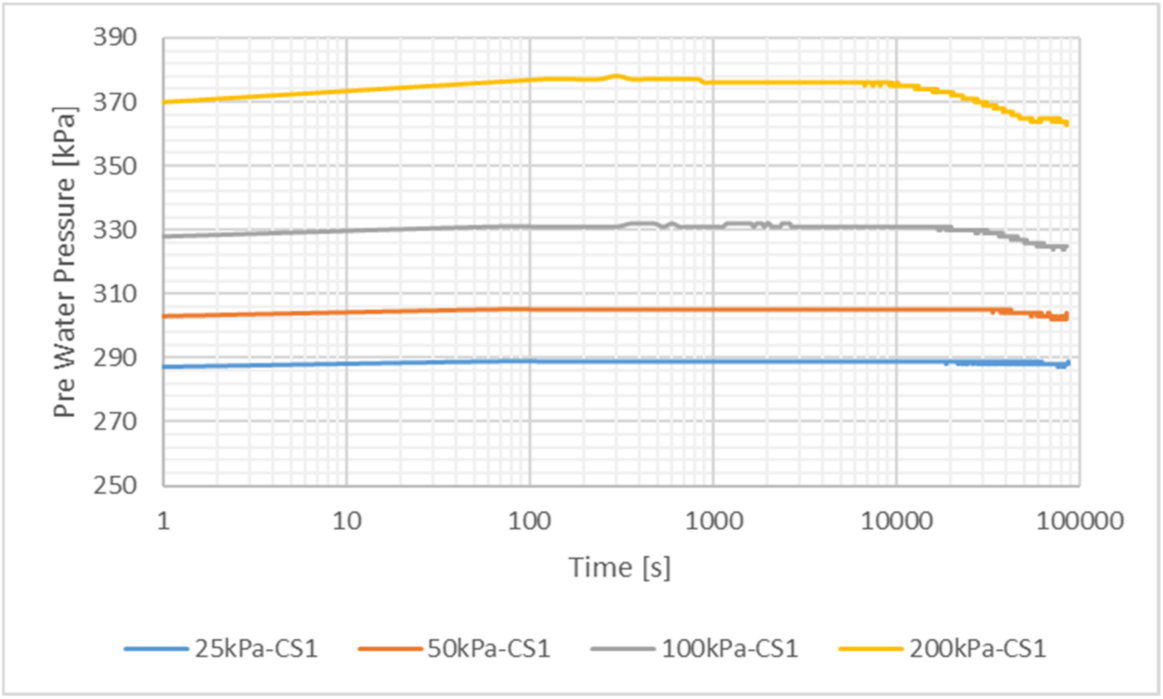

Figure 13. Pore water pressure stabilization curves for coal sludge (CS1), undrained conditions.

Analysis of the consolidation diagrams showing the change in the height of the specimens overtime after the application of successive load degrees, performed using both the Casagrande, and Taylor methods (Figure 15), indicates that the greatest vertical deformation occurred at $\sigma' = 50$ kPa ($\varepsilon_{CS1} = 0.037$, $\varepsilon_{CS2} = 0.039$, $\varepsilon_{CS1} = 0.035$). Stabilization of the increase in the settlement at $\sigma' = 50$ kPa occurred three hours after the load was applied. Despite the general similarity of the shape of the curves, it can be observed the

significant increase in settlement of the CS3 specimen at the load degree $\sigma' = 25$ kPa, and to a much larger zone of initial consolidation at the load $\sigma' = 50$ kPa, clearly visible in the graphs made with the use of Taylor's method. (Figure 15—CS3 consolidation curve-Taylor method). It indicates that the CS3 sample is more compressible. The consolidation of the material in two consecutive degrees had a very similar course in all three samples.

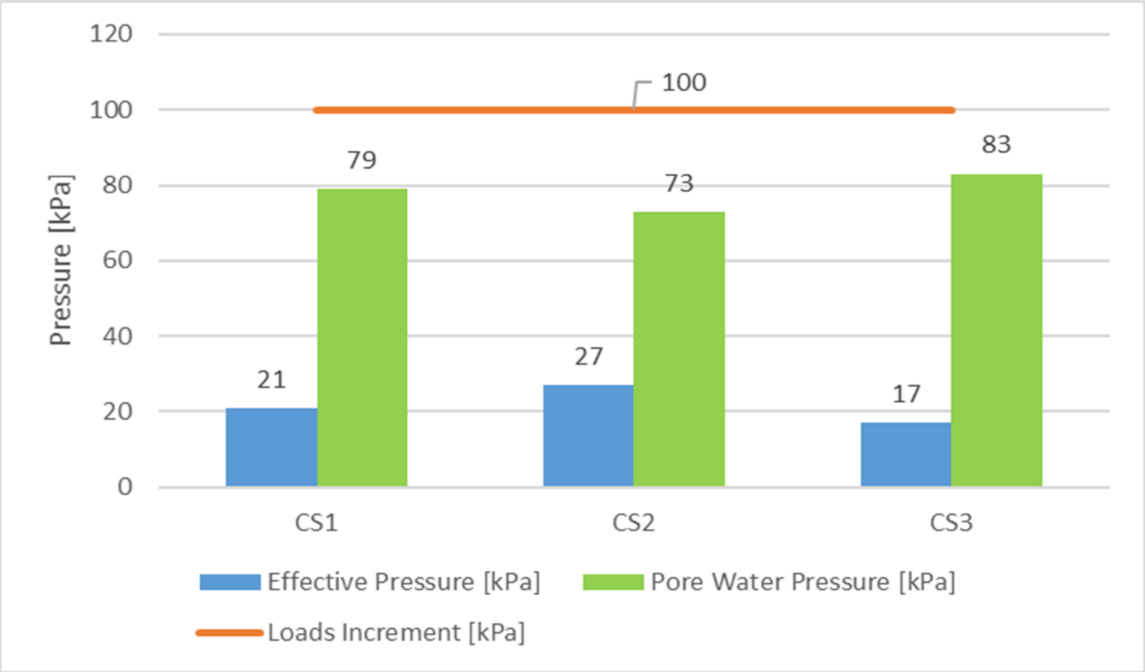

Figure 14. Pressure distribution in load increment of 100 kPa (undrained conditions).

The above analysis, the initial differences in the course of settlements, and their similar course in the further degrees of loading: $\sigma' = 100$ kPa, $\sigma' = 200$ kPa demonstrate an even distribution of the water pressure in the soil pores, resulting in the reduction in initial consolidation and stabilization phase in the course of the consolidation of the tested material.

The pore pressure distribution curves vary both within the tested sample and in the consolidation of all the samples tested (Figure 15). The initial phase of consolidation, especially consolidation at $\sigma' = 25$ kPa, draws our attention here. The outlier is sample CS2 in which, at 25 kPa, the pore pressure dissipation factor reaches its maximum value (100%) already after 1 min from the opening of the drain. In the case of CS3, maximum dissipation occurs at 7 min. Finally, in the case of CS1, total pore water pressure dissipation occurs at 80 min.

Such material behavior during consolidation may be a consequence of how the individual samples/specimens were saturated. The curves of water pressure dissipation in the soil pores indicate that the initial consolidation dominated at this stage, i.e., under the influence of the applied load, the removal of residual air took place in addition to the outflow of water. In further stages of consolidation, i.e., at effective stresses of 100 kPa, and 200 kPa, a similarity of results is observed.

A summary of the consolidation factor with its mean values and the estimated confidence interval is illustrated in Figure 16.

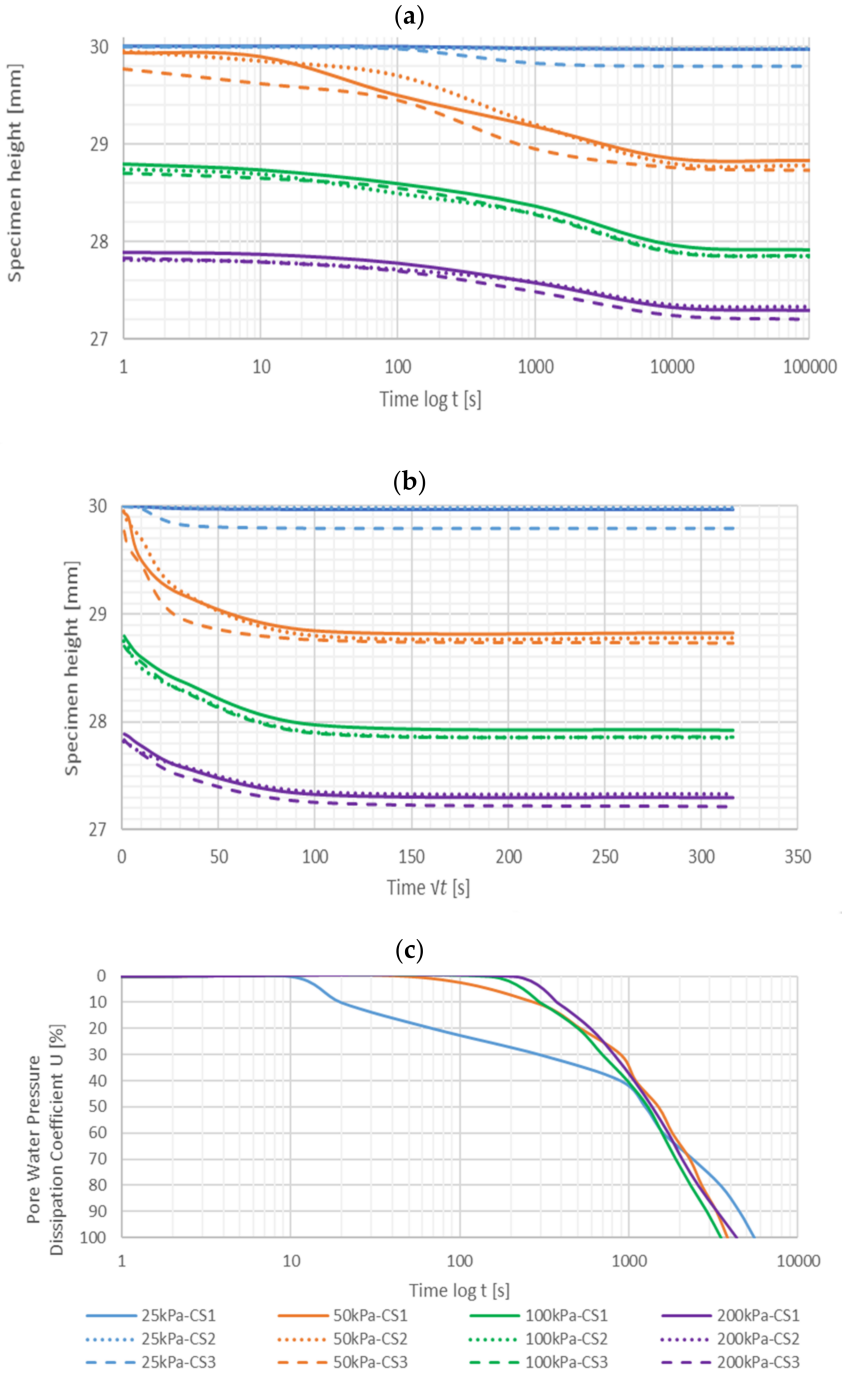

Figure 15. Coal sludge consolidation curves comparison. (**a**) The log time method (due to Casagrande) (**b**) The root time method (due to Taylor) (**c**) The pore water pressure dissipation method (due to Robbinson).

The large scatter in the values of the consolidation coefficient obtained in the first phase of the process (at $\sigma' = 25$ kPa), was due to differences in the pore pressure dissipation pattern in the individual samples during the filtration consolidation. Hence, these values were erroneous and were discarded in further analysis (e.g., in the determination of the permeability coefficient by the indirect method).

A comparison of the average values for the effective primary compressibility modulus with the values of the consolidation factor and compressibility curve are shown in Figures 17 and 18, respectively.

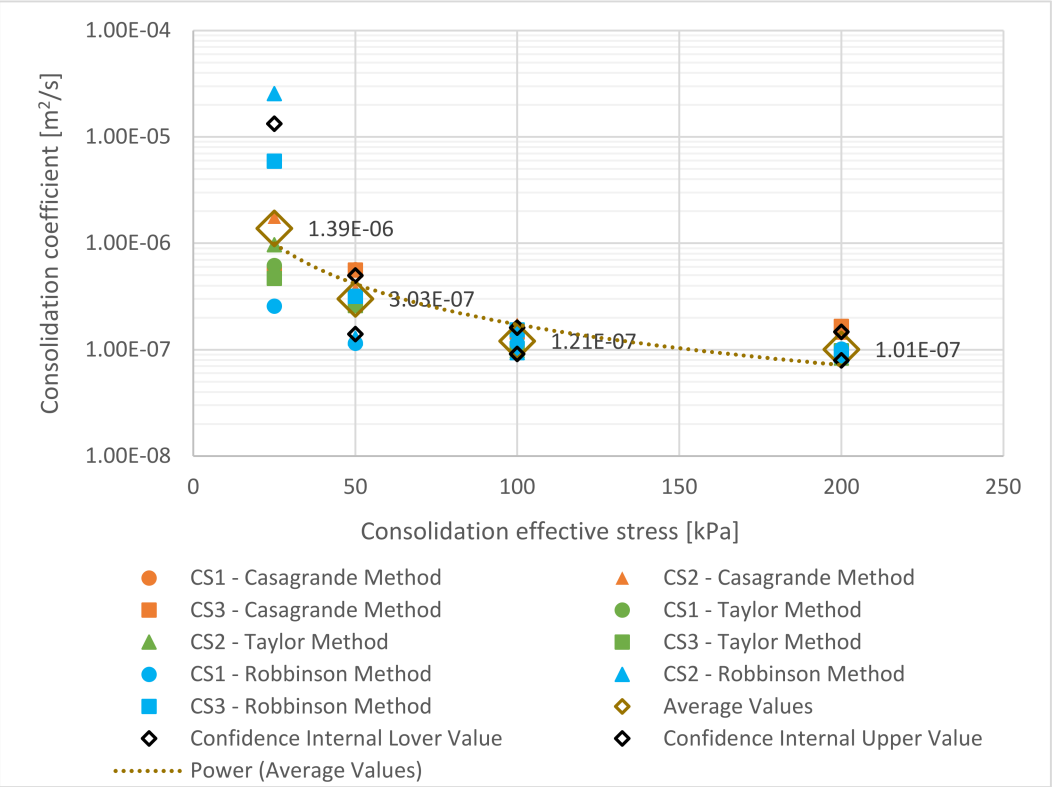

Figure 16. Consolidation coefficient values were obtained in three different determination methods.

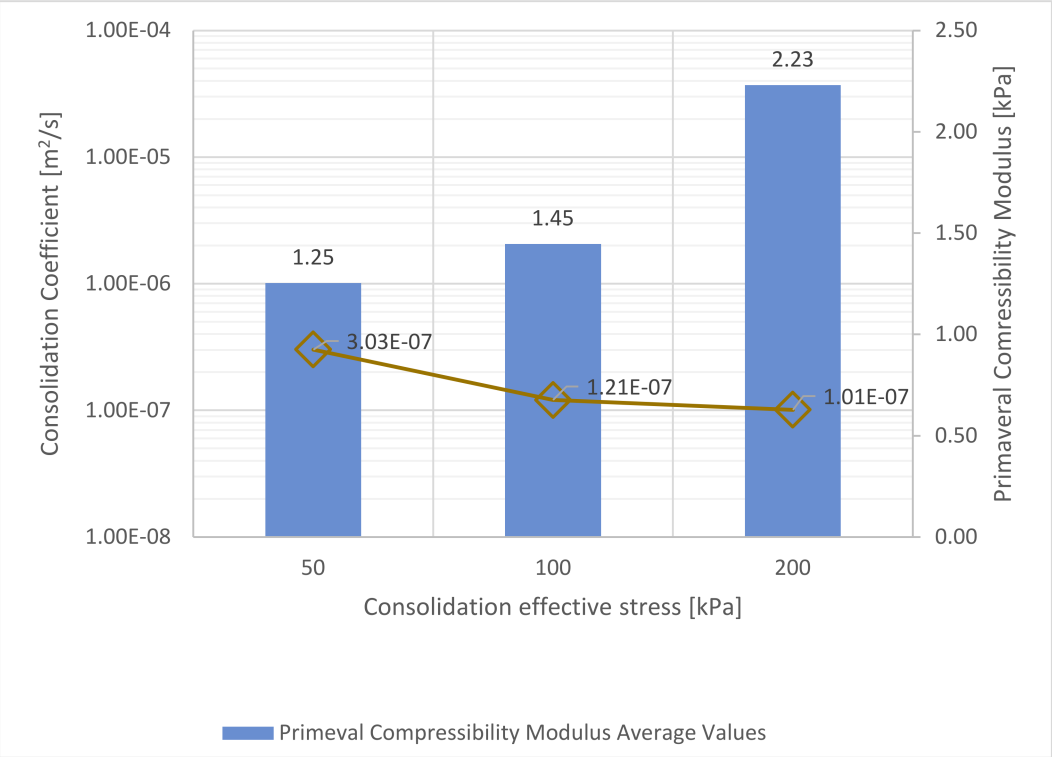

Figure 17. Compressibility parameters value changes with sample load increasing.

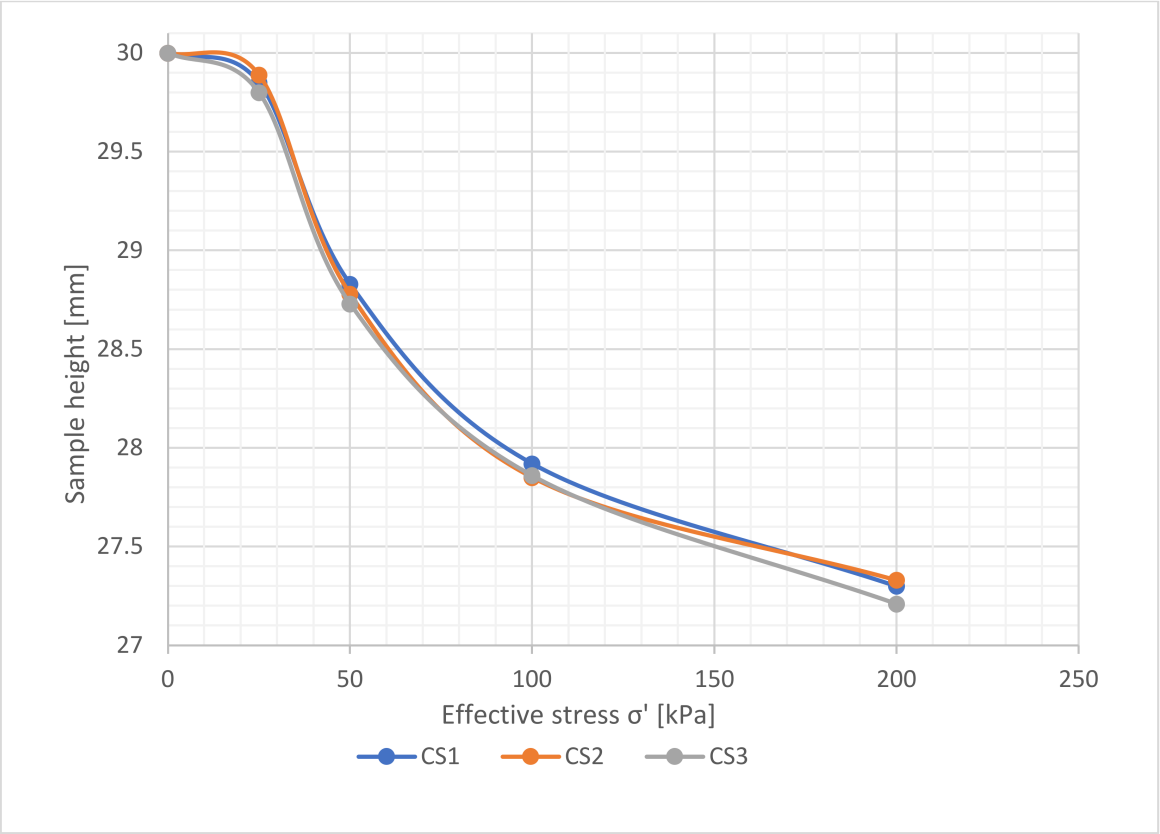

Figure 18. Compressibility curve, h = f (σ′).

4.4. Permeability

4.4.1. Indirect Method

According to the guidelines contained in Section 3, the permeability coefficient of the coal sludge was calculated from the values of the consolidation coefficient (c_v), and the primary compressibility modulus (M_0) obtained in the consolidation tests. The calculated values are summarized in Table 5.

Table 5. Summary of permeability coefficient values obtained from indirect method.

k_v $\left[\frac{m}{s}\right]$	Determination Method c_v	Consolidation Stress [kPa]		
		50 kPa	100 kPa	200 kPa
		Permeability Coefficient [m/s]		
CS1	Casagrande Method	4.27×10^{-9}	1.05×10^{-9}	6.55×10^{-10}
	Taylor Method	2.14×10^{-9}	6.53×10^{-10}	4.12×10^{-10}
	PWP Method *	8.67×10^{-9}	7.63×10^{-10}	4.44×10^{-10}
CS2	Casagrande Method	2.96×10^{-9}	1.20×10^{-9}	6.24×10^{-10}
	Taylor Method	2.15×10^{-9}	6.76×10^{-10}	3.64×10^{-10}
	PWP Method *	1.01×10^{-9}	6.47×10^{-10}	4.25×10^{-10}
CS3	Casagrande Method	4.56×10^{-9}	1.01×10^{-9}	7.45×10^{-10}
	Taylor Method	2.12×10^{-9}	7.10×10^{-10}	4.43×10^{-10}
	PWP Method *	2.59×10^{-9}	1.06×10^{-9}	3.99×10^{-10}

* Pre Water Pressure Dissipation Method.

A comparison of the average values of the permeability coefficient at successive load degrees shows that its value decreases with increasing effective stress acting on the specimen (Figure 19).

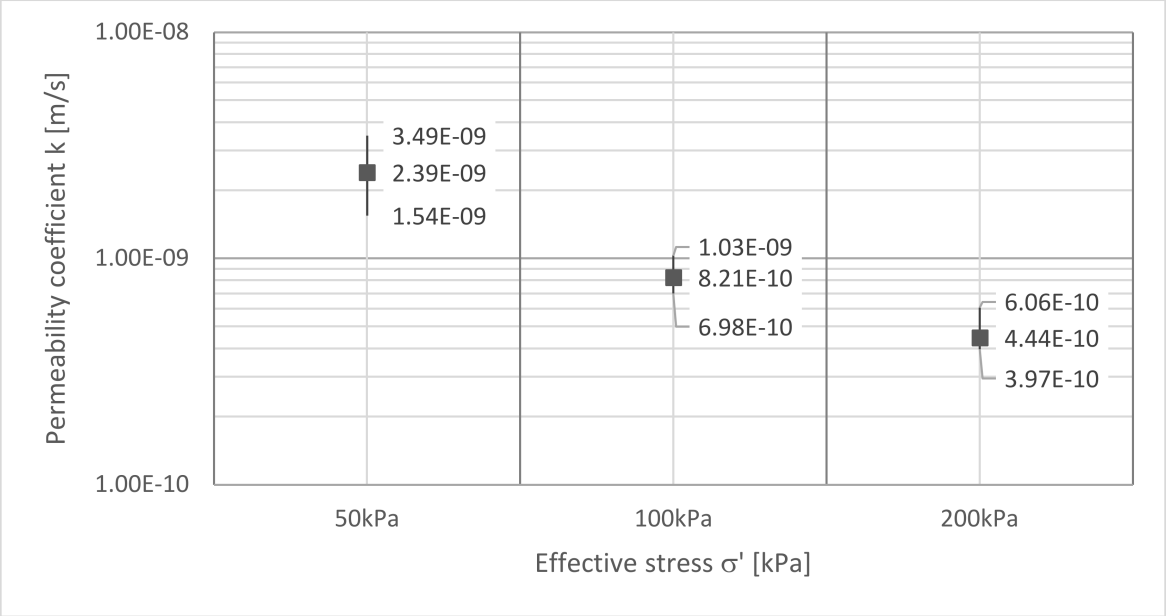

Figure 19. Average permeability coefficient values within the specified confidence interval.

4.4.2. Direct Method

In the direct method, increase the pressure gradient acting on the specimen, causing an increase in the value of the hydraulic gradient, under conditions of constant effective stress acting on the sample (variant 1), increasing the water flux flowing through the sample, and, thus, a higher value of the permeability coefficient (Figure 20).

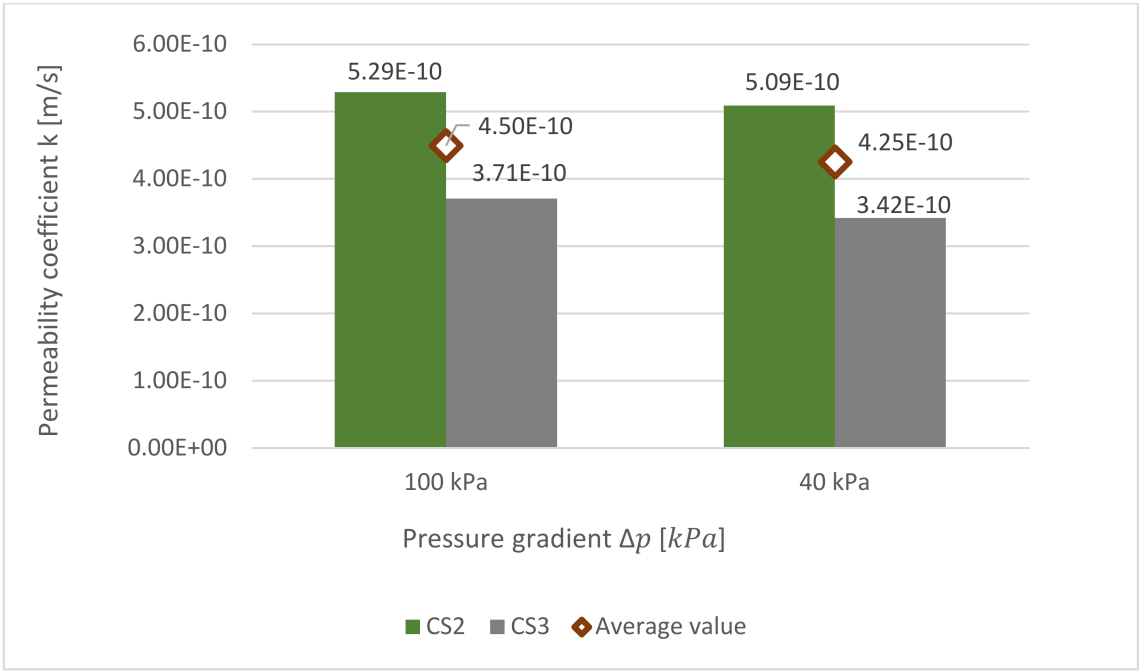

Figure 20. Dependence of the permeability coefficient value on the pressure gradient at the effective stress of 200 kPa for samples CS2, and CS3.

The second variant of the water permeability test assumed a change in effective stress value at a constant pressure gradient. For samples CS2, and CS3 the value of Δp = 40 kPa was assumed. The obtained results of the water permeability test showed that the value of the filtration coefficient also decreases with an increase in the value of effective stress at which the test was performed (Figure 21).

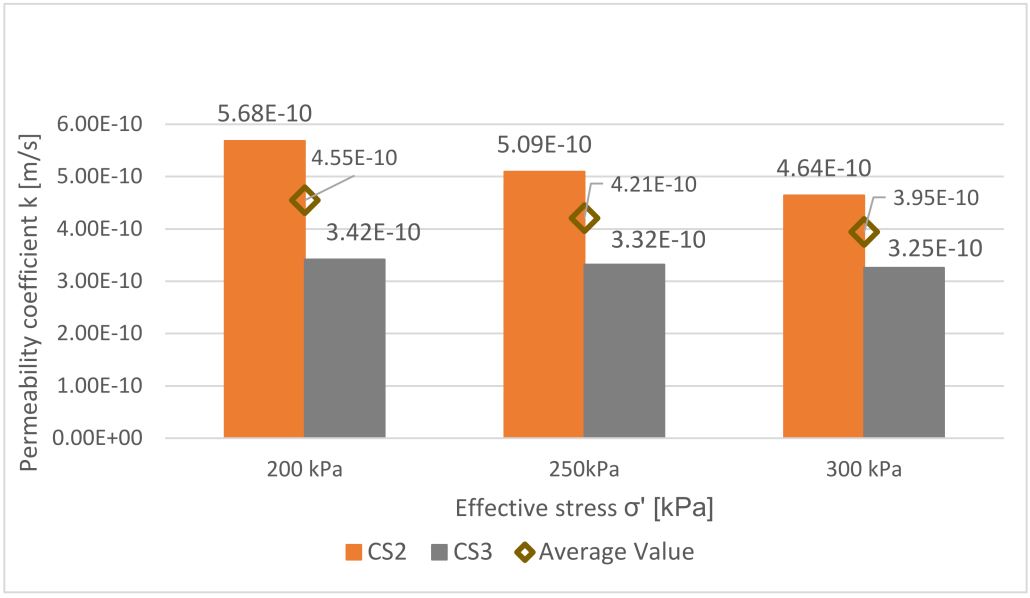

Figure 21. Dependence of the permeability coefficient value on the effective stress increases at the pressure gradient of 40 kPa for samples CS2, and CS3.

4.4.3. The Indirect and Direct Method Results Comparison

The coal sludge specimens for which the indirect method was used to calculate the filtration coefficient values were under the following effective stress values: 50 kPa, 100 kPa, and 200 kPa. It was demonstrated that as the pressure on the sample increases, the value of the parameter in question decreases. Direct water flow measurement through individual samples of coal sludge was carried out at effective stress of σ′ = 200 kPa, σ′ = 250 kPa, and σ′ = 300 kPa. The common denominator of both methods is the determinations at the effective stress of σ′ = 200 kPa, the filtration coefficient values was compared for the results of the tests carried out under the aforementioned stress.

The average values of filtration coefficients obtained by the direct method at effective stress of σ′ = 200 kPa, and the different pressure gradients of water flowing through the sample were compared with the results of this parameter obtained by the indirect method (at the same sample pressure). The indirect method gives lower values of the filtration coefficient compared to the results of the direct method, but it is still the same order of magnitude (Figure 22).

Based on the conducted test of significance (test for two variances), the values of the statistic were obtained $F < F_{\alpha}$; $(1.04 < 5.14)$, so there are no grounds to reject the hypothesis. The average value of the filtration coefficient (from indirect and direct methods) is 4.35E-10 m/s.

4.5. Summary of Research Results

Research on the characteristics of coal sludge confirmed that its properties are typical for fine-grained waste from hard coal processing [13,16,22]. Both the grain composition, chemical composition, phase composition and microscopic observations confirm the high content of the finest grains. The mineral material contents of coal sludge are, among others, kaolinite and smectite-illite packages which determine low permeability conditions, whereas quartz give some strength of CS. The LOI value is typical for this type of waste

and is correlated with the specific content of carbon grains, also found in microscopic observations. In terms of environmental properties, the coal sludge meets the legal requirements in terms of leachability [68,69], the content of trace elements and the content of radionuclides [70].

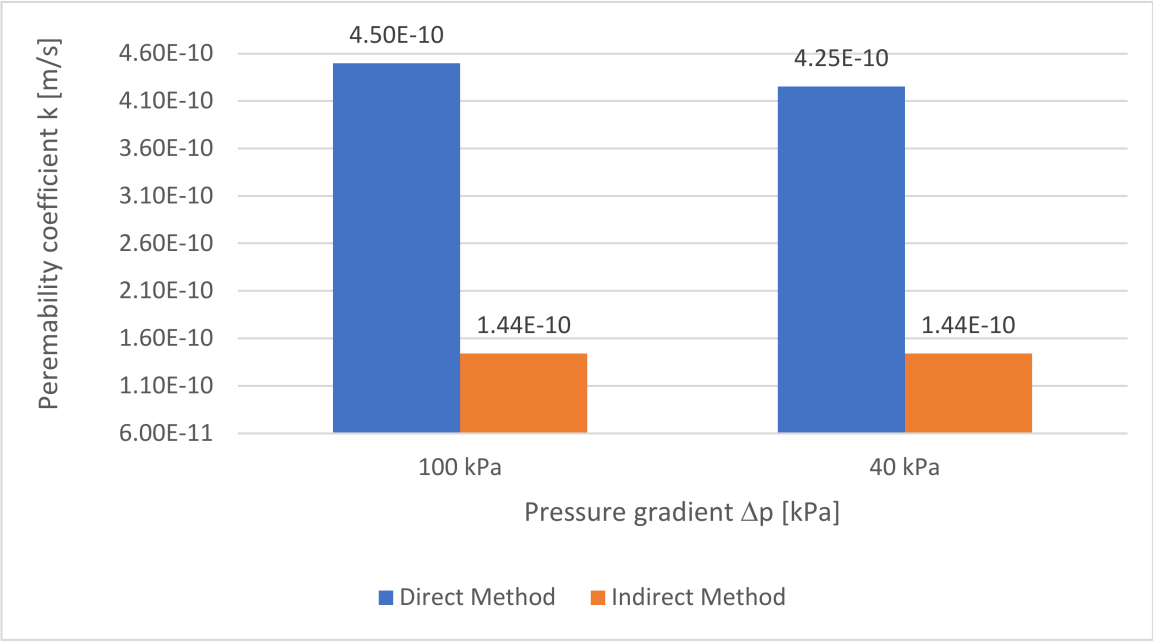

Figure 22. Permeability coefficient values comparison obtained due to direct, and indirect method.

Analysis of the saturation course of the CS samples demonstrated that the duration of the process depends on the initial saturation of the material. It is noteworthy that although the specimens were taken from the same representative sample and prepared under the same conditions, their initial water content differed significantly. The sample CS 3 took the longest to saturate, as it had the lowest initial saturation, B = 0.27. Despite the same conditions in terms of the rate of pressure build-up on the sample during the saturation process and similar values of effective stress acting on the sample, significant differences in the time of saturation for individual specimens were observed. The results of the saturation stage confirm that the Skempton parameter used in the study is a sufficient indicator for determining the degree of sample saturation. The values of this parameter reached B = 1 at different total pressures in individual samples but at constant values of effective stresses. The proper saturation of the sample, and thus the transition to a two-phase medium, greatly influences the correct course of the other processes (consolidation, and measurement of material permeability).

The process of pore water pressure equilibration in the soil in all three samples was similar, testifying to correct saturation. However, on the other hand, the comparable shape of the settlement curves, especially visible at higher loading degrees, as follows: $\sigma' = 100\ kPa$, and $\sigma' = 200\ kPa$ confirms the uniform distribution of pore water pressure and the stabilized course of the consolidation process in the material under study.

Determination of the consolidation coefficient using different methods makes it possible to eliminate erroneous results. Comparison of the values of the parameter obtained with methods involving the change of sample height in time, with the course of the pore pressure scatters curve, allows for the elimination of erroneous readings caused by the initial consolidation phase of the sample (misclassification of the results from the initial phase to the primary consolidation phase). Although each consolidated sample was previously saturated (B = 1), readings indicating the presence of some disturbance in the samples appeared during the initial consolidation phase. In the subsequent stages of consolidation, no such disorders were observed, the flow of water in the samples being laminar. The order

of magnitude for the total settlements of the individual coal sludge specimens reached a similar value.

The importance of this test is that it relates directly to the value of effective stresses, owing to the possibility of continuously measuring the pore water pressure in the material. The analysis of the filtration consolidation process based on the pore pressure dissipation factor showed the occurrence of disturbances in the consolidation process at the initial sample load degrees, which indicates a much higher sensitivity of this method. Furthermore, conducting the consolidation process in a Rowe Cell allowed us to determine the values of parameters such as the consolidation coefficient and the effective modulus of primary compressibility.

A comparison of the permeability coefficient values determined by the indirect, and direct methods showed a convergence of results, confirming the truth of the H_0 hypothesis. However, the visible scatter of the results is conditioned by the diversity of the tested material, which manifests itself by chemical composition and in other physical properties, which do not remain the subject of consideration for the article.

According to commonly accepted classifications, isolating barrier materials should have a filtration coefficient $k < 10^{-9}$ m/s [33–35]. These same requirements were also presented in Wysokiński's classification [74], where the filtration coefficient value k on the level lower than 10^{-9} m/s is one of the most important criteria for assessing the suitability of soil for the construction of mineral insulation screens. Moreover, designed mineral barriers use in landfill construction have permeability of 1×10^{-9} m/s [75]. In comparison, for mixtures of the Polish Neogene clays with dunes, as investigated by Luczak-Wilamowska [76], the coefficient of permeability for these mixtures amounted to 1.83–3.8 $\times 10^{-10}$ m/s. Correctly built mineral liners at the municipal land-fill construction are those with a coefficient of permeability less than 10^{-9} m/s [77]. The obtained value of the filtration coefficient for coal sludge ($k < 10^{-10}$ m/s) will meet these requirements. This confirms the assumptions about the possibility of using coal sludge to seal landfills, indicated, among others, by Klojzy-Kaczmarczyk, Staszczak [31].

5. Conclusions

The study aimed to investigate the permeability of coal sludge. The sealing system is one of the most important structural elements of the land-fill. Low water permeability is one of the most important parameters determining the use of a given material as mineral screens.

The obtained value of the filtration coefficient for coal sludge ($k < 10^{-10}$ m/s) allows to conclude that this material can be used to build mineral insulation layers in landfills and is safe for the environment. Hence, it is the real possibility of using coal sludge waste in geoengineering for insulting layers. However, additional geotechnical tests (such as consistency limits, shear strength properties, etc.) will be necessary to confirm the final conditions and parameters of the materials used with coal sludge for specific locations.

Supplementary Materials: The following supporting information can be downloaded at: https://www.mdpi.com/article/10.3390/min12020212/s1, Table S1: The values of parameter B at the end of the saturation process, Table S2: Methods for vertical consolidation coefficient determination.

Author Contributions: Conceptualization, J.A. and R.P.; methodology, J.A.; investigation, J.A.; writing—original draft preparation, J.A.; writing—review, and editing, R.P.; supervision, R.P. All authors have read and agreed to the published version of the manuscript.

Funding: This research received no external funding.

Acknowledgments: The tests were carried out based on AGH statutory works.

Conflicts of Interest: The authors declare no conflict of interest.

Nomenclature

The following symbols are used in this paper:

A	cross-sectional area of the sample,
B	Skempton parameter,
CS	coal sludge,
c_v	coefficient of consolidation, m^2/s
γ_w	water weight,
k	coefficient of permeability, m/s
L	sample length, m, mm
M_0	one-sided primary compressibility modulus of the soil,
m_v	volumetric compressibility factor of the soil,
pc	pressure loss in the system for flow rate q [kPa],
q	the average rate of water flow through the sample [mL/min],
Rt	temperature correction factor for water viscosity,
t	consolidation process duration time (time elapsed since the load was applied), s
u	pore water pressure after time t,
U	degree of dissipation of water pressure in the pores of the ground,
u_0	excess pore water pressure in the soil at the beginning of the consolidation phase,
u_1	pore water pressure at the beginning of the consolidation process,
u_2	pore pressure in the soil at the end of the consolidation phase,
u_t	excess water pressure in the soil pores during consolidation time t,
Δu	increase in pore water pressure in the soil [kPa],
$\Delta\sigma_u$	increment of vertical consolidation pressure [σ_u kPa],
Uz	degree of consolidation,
Δp = (p1 − p2)	the difference between the pressure of water entering the sample, and the pressure of water leaving it [kPa].

References

1. Skarżyńska, K.M. Reuse of coal mining waste in civil engineering–part 1: Properties of minestone. *Waste Manag.* **1995**, *15*, 2–42. [CrossRef]
2. Zawisza, E. Wpływ zagęszczenia i wilgotności na wytrzymałość na ścinanie wybranych odpadów przemysłowych i gruntu mineralnego (Influence of compaction and humidity on shear strength of selected industrial waste and mineral soil, Polish). *Przegląd Górniczy* **2006**, *62*, 27–32.
3. Kuranchie, F.A.; Shukla, S.K.; Habibi, D. Mine wastes in Western Australia and their suitability for embankment construction. In Proceedings of the Geotechnical Special Publication, San Diego, CA, USA, 3–7 March 2013; pp. 1443–1452.
4. Amrani, M.; Taha, Y.; El Haloui, Y.; Benzaazoua, M.; Hakkou, R. Sustainable Reuse of Coal Mine Waste: Experimental and Economic Assessments for Embankments and Pavement Layer Applications in Morocco. *Minerals* **2020**, *10*, 851. [CrossRef]
5. Banerjee, L.; Chawla, S.; Kumar Dash, S. Application of geocell reinforced coal mine overburden waste as subballast in railway tracks on weak subgrade. *Constr. Build. Mater.* **2020**, *265*, 120774. [CrossRef]
6. Chugh, Y.P.; Behum, P.T. Coal waste management practices in the USA: An overview. *Int. J. Coal Sci. Technol.* **2014**, *1*, 163–176. [CrossRef]
7. Fan, G.; Zhang, D.; Wang, X. Reduction and utilization of coal mine waste rock in China: A case study in Tiefa coalfield. Resources. *Conserv. Recycl.* **2014**, *83*, 24–33. [CrossRef]
8. Gruchot, A.; Zawisza, E. Zagęszczalność i nosność wybranych odpadów powęglowych i pohutniczych Compactability and bearing capacity of selected coal and metallurgical waste. *Przegląd Górniczy* **2007**, *63*, 26–30.
9. Adamczyk, J. Basic geotechnical properties of mining, and processing waste–a state of the art analysis. *AGH J. Min. Geoengin.* **2012**, *36*, 31–41.
10. Gruchot, A. Wskaźnik nosnosci CBR kompozytów z odpadów powęglowych i popiołu lotnego. *Przegląd Górniczy* **2014**, *2*, 12–17.
11. Baic, I.; Blaschke, W.; Szafarczyk, J. Deposits of coal sludge as a source of energy fuel-information on the development project. *Przegląd Górniczy* **2010**, *1*, 73.
12. Hycnar, J.; Fraś, A.; Przystać, R.; Foltyn, R. Opportunities to improve the quality of coal sludge for power generation, and industry. *Ind. FurnancesBoilers* **2015**, *2*, 17–25.
13. Tora, B.; Pasiowiec, P.; Hycnar, J.J. Fine Coal Waste Utilisation. *Inżynieria Miner.—J. Pol. Miner. Eng. Soc.* **2016**, *37*, 213–222.
14. Biernatowski, K.; Rybak, C.; Sarniak, W. *Foundation Engineering. A Guide to Designing*; Wydawnictwo Politechniki Wrocławskiej: Wrocław, Poland, 1972.

15. Taha, Y.; Benzaazoua, M.; Hakkou, R.; Mansori, M. Coal mine wastes recycling for coal recovery and eco-friendly bricks production. *Miner. Eng.* **2017**, *107*, 123–138. [CrossRef]
16. Vasić, M.V.; Goel, G.; Vasić, M.; Radojević, Z. Recycling of waste coal dust for the energy-efficient fabrication of bricks: A laboratory to industrial-scale study. *Environ. Technol. Innov.* **2021**, *21*, 101350. [CrossRef]
17. Łabaj, J.; Blacha, L.; Smalcerz, A.; Wieczorek, J.; Fröhlichová, M.; Vadasz, P.; Findorak, R.; Niesler, M. Utilization of waste coal flotation concentrate for copper matte smelting. *Eng. Sci. Technol. Int. J.* **2021**, *24*, 996–1004. [CrossRef]
18. Pomykała, R.; Kępys, W. The properties of the backfill mixtures based on own fine-grained waste. In *Minefill 2020–2021*; CRC Press: Boca Raton, FL, USA, 2021.
19. Klojzy-Karczmarczyk, B.; Mazurek, J.; Paw, K. Możliwości zagospodarowania kruszyw i odpadów wydobywczych górnictwa węgla kamiennego ZG Janina w procesach rekultywacji wyrobisk odkrywkowych. *Gospod. Surowcami Miner.* **2016**, *32*, 111–134. [CrossRef]
20. Grela, A.; Łach, M.; Bajda, T.; Mikuła, J. Alkaliczna aktywacja popiołów po spalaniu mułów węglowych. *Zesz. Nauk. Inst. Gospod. Surowcami Miner. I Energią PAN Rok* **2016**, *95*, 181–192.
21. Stankiewicz, J.; Góralczyk, S. Kierunki gospodarczego wykorzystania odpadów po procesach wzbogacania depozytów mułów węglowych. *Czas. Tech.* **2012**, *63*.
22. Baic, I. Analysis of the Chemical, Physical and Energetic Parameters of Coal Sludge Deposits Inventoried in the Silesian Province. *Annu. Set Environ. Prot.* **2013**, *15*, 1525–1548. (In Polish)
23. Alam, S.; Das, S.K.; Rao, B.H. Strength, and durability characteristic of alkali activated GGBS stabilized red mud as geo-material. *Constr. Build. Mater.* **2019**, *211*, 932–942. [CrossRef]
24. Liu, J.P.; Lu, Y.S.; Bai, X.H.; He, B. Mechanical properties, and strength mechanism of coal metakaolin-bayer red mud complex. *Fresenius Environ. Bull.* **2020**, *29*, 8610.
25. Wichliński, M.; Kobylecki, R.; Bis, Z. Badania zawartości rtęci w mułach węglowych (Tests of mercury content in coal sludge; Polish). *Polityka Energetyczna* **2016**, *19*, 115–124.
26. Liew, M.; Xiao, M.; Liu, S.; Rudenko, D. In Situ Seismic Investigations for Evaluating Geotechnical Properties, and Liquefaction Potential of Fine coal Tailings. *J. Geotech. Geoenviron. Eng.* **2020**, *146*, 04020014. [CrossRef]
27. Islam, S.; Williams, D.J.; Zhang Ch Liano-Serna, M. Geotechnical characterization of coal tailings down the beach, and constant rate of loading consolidation in a slurry consolidometer. *Min. Technol.* **2021**, *130*, 67–80. [CrossRef]
28. Doniecki, T.; Siedlecka, E. Waste coal sludge as an element of mineral insulation of landfills. *Min. Geoengin.* **2006**, *30*, 41–46.
29. Sajjad, S.; Xiao, M.; Khosravifar, A.; Liew, M.; Liu, S.; Rostami, J. Characterization of static, and dynamic geotechnical properties, and behaviors of fine coal refuse. *Can. Geotech. J.* **2019**, *56*, 12. [CrossRef]
30. Yu, H.; Zeng, X.; Michael, P.R. Geotechnical Properties, and flow Behavior of Coal Refuse, and Static, and Impact Loading. *J. Geotech. Geoenviron. Eng.* **2019**, *145*, 04019024. [CrossRef]
31. Klojzy-Kaczmarczyk, B.; Staszczak, J. The use of coal sludge to isolation municipal landfills-recognition of the possibility. *Zesz. Nauk. Inst. Gospod. Surowcami Miner. Pol. Akad. Nauk.* **2018**, *105*, 95–108.
32. Doniecki, T.; Siedlecka, E. Variability of filtration coefficient in coal sludge proposed for construction of isolation barriers. *Eng. Environ. Prot.* **2009**, *12*, 219–230.
33. Witczak, S.; Adamczyk, A. *A Catalogue of Selected Physical, and Chemical Coefficients for Underground Waters Contamination, and the Methods to Determine such Ones*; Biblioteka Monitoringu Środowiska: Warsaw, Poland, 1994.
34. Dowgiałło, J.; Kozerski, B.; Krajewski, S.; Macher, J.; Macioszczyk, T.; Malinowski, J.; Paczyński, B.; Płochniewski, Z.; Stenzel, P.; Szymanko, J.; et al. *A Guidebook for Hydrogeologist*; Wydawnictwo Geologiczne: Warsaw, Poland, 2007.
35. Gavich, I.K. Teoreticheskiye osnowy izuczenija dwiżenija podziemnych wod v zemnoj kore. In *Osnovy gidrogeologii, T.II: Gidrogeodinamika*; Zekcer, I.S., Ed.; Izdatelstvo Nauka: Novosybirsk, Russia, 1983.
36. Szymański, A. *Mechanics of Soils*; SGGW Publishing House: Warsaw, Poland, 2007.
37. Das, B.M. *Fundamentals of Geotechnical Engineering*; Brooks/Cole Thomson Learning: Stanford, CA, USA, 2000.
38. Craig, R.F. *Soil Mechanics*; Taylor & Francis e-Library: Dundee, UK, 2004.
39. Olek, B.; Woźniak, H. Determination of quasi-filtration phase of consolidation based on experimental, and theoretical course of the uniaxial deformation, and distribution of pore pressure. *Geol. Geophys. Environ.* **2016**, *42*, 353–363. [CrossRef]
40. Jastrzębska, M.; Kalinowska-Pasieka, M. Selected research methods in a modern geotechnical laboratory. In *From Subsoil to Ground Parameters*; Publishing House of the Silesian University of Technology: Gliwice, Poland, 2015.
41. *ISO/TS 17892-5:2004*; Geotechnical Investigation, and Testing-Laboratory Testing of Soil-Part 5: Incremental Loading Oedometer Test. ISO: Geneva, Switzerland, 2004.
42. Gruchot, A.; Zawisza, E.; Gubała, S. Badania wytrzymałości na ścinanie odpadów powęglowych z KWK, Wesoła w aparacie trójosiowego ściskania. *Przegląd Górniczy* **2009**, *65*, 73–78.
43. *BS 1377-6 1990*; Methods of Test for Soils for Civil Engineering Purposes-Part 6: Consolidation, and Permeability Tests in Hydraulic Cells, and with Pore Pressure Measurement. Road Engineering Standards Policy Committee: London, UK, 1990.
44. Lambe, T.W.; Whitman, R.V. *Soil Mechanics*; Arkady: Warsaw, Poland, 1978.
45. Malinowska, E.; Bursa, B.; Chmielnicki, P.; Dziuba, W. Determination of vertical, and horizontal consolidation coefficient in weak-bearing organic soils. *Architectura* **2013**, *12*, 63–74.

46. Casagrande, A.; Fadum, R.E. *Notes on Soil Testing for Engineering Purposes*; Harvard Soil Mechanics Series; No. 8; Harvard University, Graduate School of Engineering: Cambridge, MA, USA, 1940; p. 71.
47. Taylor, D.W.; Merchant, W. A theory of clay consolidation accounting for secondary compression. *J. Math. Phys.* **1940**, *19*, 167–185. [CrossRef]
48. Malinowska, E.; Szymański, A.; Sas, W. Determination of flow characteristics for organis soil by flow-pump method. In *Przegląd Naukowy Inżynieria i Kształtowanie Środowiska*; Wydawnictwo Szkoły Głównej Gospodarstwa Wiejskiego w Warszawie: Warsaw, Poland, 2005.
49. Wiłun, Z. *Zarys Geotechniki*; Wydawnictwa Komunikacji i Łączności WKŁ: Warszawa, Poland, 1987.
50. Pazdro, Z. *General Hydrogeology*; Wydawnictwo Geologiczne: Warsaw, Poland, 1983.
51. McDowell, G.; de Bono, J. Relating Hydraulic Conductivity to Particle Size Using DEM. *Int. J. Geomech* **2021**, *21*, 06020034. [CrossRef]
52. Carrier, W.D., III. Goodbye, Hazen; Hello, Kozeny-Carman. *J. Geotech. Geoenviron. Eng.* **2003**, *129*, 1054–1056. [CrossRef]
53. Pliakas, F.; Petalas, C. Determination of Hydraulic conductivity of Unconsolidates River Alluvium from Permameter Tests, Empirical formulas, and Statistical Parameters Effect Analysis. *Water Resour. Manag.* **2011**, *25*, 2877–2899. [CrossRef]
54. Riha, J.; Petrula, L.; Hala, M.; Alhasan, Z. Assessment of empirical formulae for determining the hydraulic conductivity of glass beads. *J. Hydrol. Hydromech.* **2018**, *66*, 337–347. [CrossRef]
55. Shamsuddin, M.K.N.; Sulaiman, W.N.A.; Ramli, M.F. Vertical hydraulic conductivity of riverbank, and hyporheic zone sediment at Muda River riverbank filtration site, Malaysia. *Appl. Water Sci.* **2019**, *9*, 8. [CrossRef]
56. Odong, J. Evaluation of Emirical Formulae for Determination of Hydraulic conductivity based on Gran-size Analysis. *J. Am. Sci.* **2007**, *3*, 54–60.
57. Eggleston, J.; Rojstaczer, S. The Value of Grain-size Hydraulic Conductivity Estimates: Comparision with High Resolution In-situ Field Hydraulic Conductivity. *Geophys. Res. Lett.* **2001**, *28*, 4255–4258. [CrossRef]
58. Świrska, J. Estimation of the Filtration Coefficients for Granular Materials. In *Roczniki Inżynierii Budowlanej*; Komisja Inżynierii Budowlanej Oddział Polskiej Akademii Nauk w Katowicach: Katowice, Poland, 2009; Volume 9.
59. Cheng, C.; Song, J.; Chen, X.; Wang, D. Statistical Distribution of Streambed Vertical Hydraulic Conductivity along the Platte river, Nebraska. *Water Resour. Manag.* **2011**, *25*, 265–285. [CrossRef]
60. Gruchot, A.T.; Zydroń, E.; Zawisza, E.; Szałucha, Ł. Analysis of filtration processes by earth hydrotechnical structures. *Acta Sci. Pol. Form. Circumiectus* **2019**, *18*, 39–50. [CrossRef]
61. Koś, K.; Gruchot, A.; Zawisza, E. Bottom Sediments from a Dam Reservoir as a Core in Embankments-Filtration, and Stability: A Case Study. *Sustainability* **2021**, *13*, 1221. [CrossRef]
62. Olek, B.S. Experimental insights into consolidation rates during one-dimentional loading with special reference to excess pore water pressure. *Acta Geotech.* **2020**, *15*, 3571–3591. [CrossRef]
63. Malinowska, E.; Hyb, M. Determination of Filtration Coefficient Based on Laboratory Tests, Department of Geoengineering, Warsaw University of Life Sciences: Warsaw, Poland. Available online: www.kg.sggw.pl (accessed on 22 December 2021).
64. Marciniak, M.; Przybyłek, J.; Herzig, J.; Szczepańska, J. *Investigations of the Filtration Coefficient of Semi-Permeable Formations*; Sorus: Poznan, Poland, 1999.
65. Pisarczyk, S.; Rymsza, B. *Laboratory, and Field Studies of Soils*; Oficyna Wydawnicza Politechniki Warszawskiej: Warsaw, Poland, 1993.
66. *EN 13286-2:2010*; Unbound and Hydraulically Bound Mixtures—Part 2: Test Methods for Laboratory Reference Density and water–Proctor Compaction. European Committee for Standardization: Brussels, Belgium, 2010.
67. *EN 12457-4:2010*; Characterization of Waste Leaching Compliance test for Leaching of Granular Waste Materials and Sludges. Part 4: One Stage Batch Test at a Liguid to Solid Ratio of 1l/kg for Materials with Particle Size below 10 mm (without or with Size reduction). European Committee for Standardization: Brussels, Belgium, 2010.
68. Regulation of the Minister of the Environment on the method of assessing the pollution of the Earth's Surface. *J. Laws* **2016**. item 1395.
69. Regulation of the Minister of the Environment on the conditions to be met when discharging sewage into waters or into the ground, and on substances particularly harmful to the aquatic environment. *J. Laws* **2014**. item 1800.
70. Regulation of the Council of Ministers on the requirements for the content of natural radioactive isotopes of potassium K-40, radium Ra-226 and thorium Th-228 in raw materials and materials used in buildings intended for the stay of people and livestock, as well as in industrial waste used in construction, and control of the content of these isotopes is defined by two activity indicators. *J. Laws* **2007**. No. 4, item 29.
71. *User Guide: Rowe Cell System*; Version 2; VJ Tech Ltd.: Berkshire, UK, 2016.
72. *EN ISO 14688-2*; Geotechnical Investigation, and Testing—Identification, and Classification of Soil—Part 2: Principles for a Classification. ISO: Geneva, Switzerland, 2017; Technical Committee ISO/TC 182, Geotechnics.
73. Adamczyk, J. Assessment of Aggregate and Coal Sludge Waste Mixtures in Earthworks Application. PhD Thesis, AGH University of Science and Technology, Krakow, Poland, 2019.
74. Wysokiński, L. *Rules for the Construction of Waste Landfills, Building Research Institute, Instructions, Guidelines, Guides no 444/2009*; Instytut Techniki Budowlanej: Warsaw, Poland, 2009.

75. Darkin, M.G.; Gilpin, C.; Sangha, C.M. Direct wet surface imaging of an anaerobic biofilm by environmental scanning electron microscopy: Application to landfill clay liner barriers. *Scanning* **2001**, *23*, 346–350. [CrossRef] [PubMed]
76. Luczak-Wilamowska, B. Neogene clays from Poland as mineral sealing barriers for landfills: Experimental study. *Appl. Clay Sci.* **2020**, *21*, 22–43. [CrossRef]
77. Zabielska-Adamska, K.; Wasil, M. Tensile Strength of Barrier Material. In Proceedings of the 10th International Conference of Environmental Engineering (10th ICEE), Vilnius, Lithuania, 27–28 April 2017.